Title

Methane clumped isotopes: Progress and potential for a new isotopic tracer

Authors

Douglas, Peter MJ
Stolper, Daniel A
Eiler, John M
et al.

Publication Date

2017-11-01

DOI

10.1016/j.orggeochem.2017.07.016

Peer reviewed

Methane clumped isotopes: Progress and potential for a new isotopic tracer

Peter M. J. Douglas[ab] Daniel A. Stolper[ac] John M. Eiler[a] Alex L. Sessions[a] Michael Lawson[d] Yanhua Shuai[ae] Andrew Bishop[f] Olaf G. Podlaha[g] Alexandre A. Ferreira[h] Eugenio V. Santos Neto[h] Martin Niemann[i] Arne S. Steen[j] Ling Huang[e] Laura Chimiak[a] David L. Valentine[k] Jens Fiebig[l] Andrew J. Luhmann[m] William E. Seyfried Jr.[n] Nami Kitchen[a]

Abstract

The isotopic composition of methane is of longstanding geochemical interest, with important implications for understanding petroleum systems, atmospheric greenhouse gas concentrations, the global carbon cycle, and life in extreme environments. Recent analytical developments focusing on multiply substituted isotopologues (‘clumped isotopes’) are opening a valuable new window into methane geochemistry. When methane forms in internal isotopic equilibrium, clumped isotopes can provide a direct record of formation temperature, making this property particularly valuable for identifying different methane origins. However, it has also become clear that in certain settings methane clumped isotope measurements record kinetic rather than equilibrium isotope effects. Here we present a substantially expanded dataset of methane clumped isotope analyses, and provide a synthesis of the current interpretive framework for this parameter. In general, clumped isotope measurements indicate plausible formation temperatures for abiotic, thermogenic, and microbial methane in many geological environments, which is encouraging for the further development of this measurement as a geothermometer, and as a tracer for the source of natural gas reservoirs and emissions. We also highlight, however, instances where clumped isotope derived temperatures are higher than expected, and discuss possible factors that could distort equilibrium formation temperature signals. In microbial methane from freshwater ecosystems, in particular, clumped isotope values appear to be controlled by kinetic effects, and may ultimately be useful to study methanogen metabolism.

Keywords: Methane, Clumped isotopes, Geothermometry, Petroleum systems, Biogeochemistry

1. Introduction

Methane (CH_4) is an important component of the Earth’s carbon cycle. As the primary constituent of natural gas (~90%; (Hunt, 1979), methane extracted from geological reservoirs accounts for approximately 20% of total global energy use (IEA, 2015). Methane is also the second most important long-lived (i.e., excluding water vapor) atmospheric greenhouse gas, and on a molar basis traps 28 times as much heat as carbon dioxide on 100-year timescales (Myhre et al., 2013). More generally, as one of the most common fluid forms of organic carbon, methane has played an important role throughout Earth history, both in facilitating the movement of reduced

carbon between different environments, and as a metabolite for biotic communities. It has often been suggested that methane played a role in the origin of life on Earth (Urey, 1952, Russell et al., 2010, McCollom and Seewald, 2013), and could be a signal of life on other planets (Formisano et al., 2004, Krasnopolsky et al., 2004, Atreya et al., 2007).

Given the importance of methane, methods for identifying formation processes and transport mechanisms are of great value. In particular, the isotopic composition of methane, including both stable (i.e., $^{13}C/^{12}C$ and D/H ratios) and radioactive isotopes (i.e., ^{14}C and T), has been widely used as a tracer for sources and sinks (Martell, 1963, Schoell, 1980, Whiticar et al., 1986, Lowe et al., 1988, Quay et al., 1999, Whiticar, 1999). For example, methane produced by the thermal breakdown of organic matter during oil and gas formation generally has $^{13}C/^{12}C$ ($\delta^{13}C$) and D/H (δD) ratios higher than methane produced by microorganisms (Schoell, 1980, Whiticar et al., 1986) (Fig. 1). In addition, different pathways of microbial methanogenesis are thought to produce distinctive isotopic fractionations. Methane produced via CO_2 reduction (or hydrogenotrophic methanogenesis) shows especially low $\delta^{13}C$ values, and methane produced by fermentation (or fermentative methanogenesis) has particularly low δD values (Whiticar et al., 1986, Whiticar, 1999) (Fig. 1). Finally, abiotic methane can be generated over a wide range of temperatures by magmatic and gas–water–rock reactions that do not directly involve organic matter or microbes (Etiope and Sherwood Lollar, 2013, Etiope and Schoell, 2014). Until a few years ago, and based on limited data, the isotopic composition of abiotic gas was considered to be typically enriched in ^{13}C, with $\delta^{13}C$ values higher than −25‰. More recent data indicates that $\delta^{13}C$ values of abiotic methane in serpentinized ultramafic rocks can be as light as −37‰ and abiotic methane from Precambrian shields can be even lighter (Etiope and Sherwood Lollar, 2013).

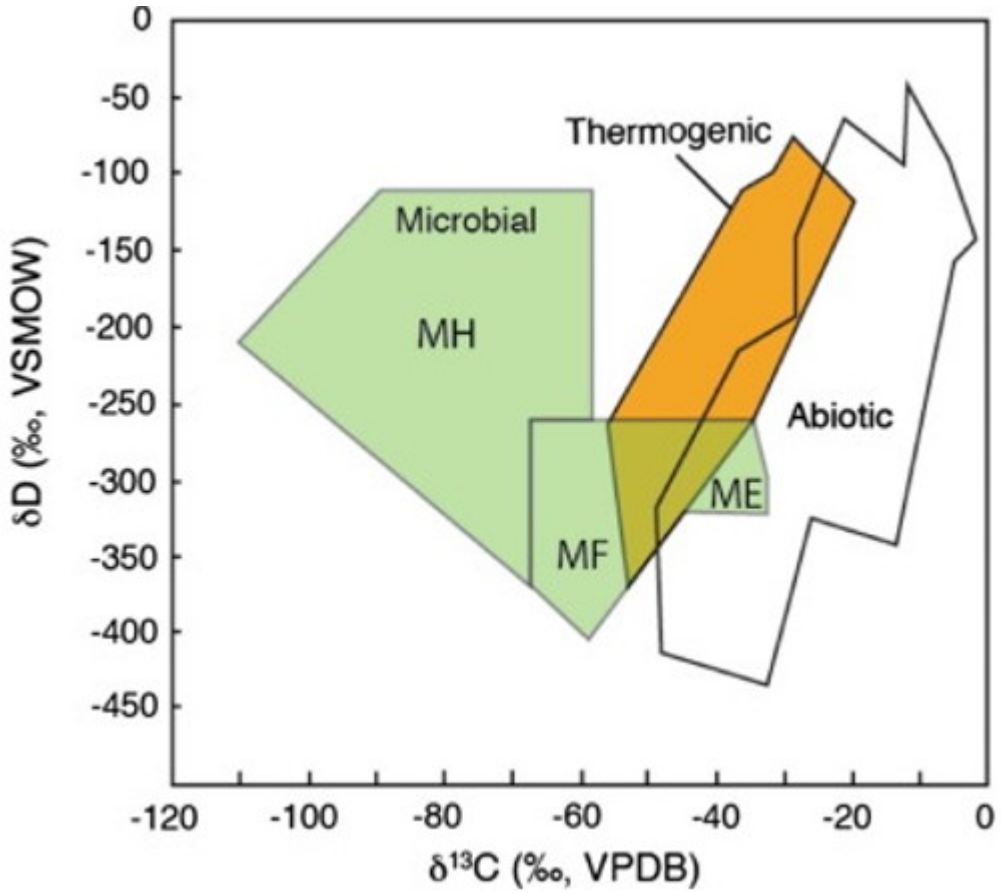

Fig. 1. Plot comparing methane $\delta^{13}C$ and δD values, after Etiope (2015) and Etiope and Sherwood Lollar (2013), based on Schoell (1980) and new empirical data. MH – microbial hydrogenotrophic; MF – microbial fermentation; ME – microbial in evaporitic environments.

Post-generation processes can also impart notable isotopic fractionations in methane. For instance, biological methane oxidation leads to an increase in both $\delta^{13}C$ and δD (Alperin et al., 1988, Whiticar, 1999) of the residual methane, while atmospheric reactions involving OH^- or Cl^- that consume methane lead to a large increase in D/H ratios in the residual gas(Gierczak et al., 1997, Saueressig et al., 2001). Diffusion of methane through a gas phaseresults in lower $\delta^{13}C$ and δD values of the gas that has diffused and elevated values in the remaining methane (Krooss et al., 1992, Zhang and Krooss, 2001, Chanton, 2005).

While conventional stable isotope ratios often provide valuable clues about methane sources and sinks, several factors limit their diagnostic ability. The empirically defined fields for $\delta^{13}C$ and δD values of different methane sources (Fig. 1) are not sharply defined, and there are clear cases of overlap between them (Martini et al., 1996, Prinzhofer and Pernaton, 1997, Martini et al., 1998, Horita and Berndt, 1999, Valentine et al., 2004, Etiope and Schoell, 2014). Moreover, a number of studies have questioned whether the isotopic fields associated with hydrogenotrophic and fermentative methane on this plot are indicative of those pathways, or of environmental or biological variables (Sugimoto and Wada, 1995, Waldron et al., 1998, Waldron et al.,

1999, Conrad, 2005, Penning et al., 2005). Finally, differentiating the effects of generation and post-generation fractionations, combined with mixing of two or more methane sources with different isotopic compositions, can be challenging (Prinzhofer and Pernaton, 1997, Martini et al., 1998, Whiticar, 1999). Combining methane stable isotope data with gas concentration or radiocarbon (^{14}C) data, or with stable isotope measurements of co-occurring phases such as water, H_2, CO_2, or ethane, can often help to resolve these ambiguities (Bernard et al., 1978, James, 1983, Coleman et al., 1995, Hornibrook et al., 1997, Waldron et al., 1999, Townsend-Small et al., 2012). Nevertheless, there is a clear need for additional tracers to help differentiate between various sources and post-generation processes.

The clumped isotope composition of methane has great potential to complement conventional measurements including both isotopic and gas composition measurements. ‘Clumped isotope’, as used here, refers to molecules with two or more rare, generally heavy stable isotopes (Eiler, 2007, Eiler, 2013). For methane, this implies either a ^{13}C and one or more D substitutions, or two or more D substitutions, in the same molecule. For a population of methane molecules that are in isotopic equilibrium with one another, the abundance of multiply-substituted isotopologues relative to a stochastic (random) distribution is a function of temperature (Stolper et al., 2014a, Webb and Miller, 2014, Wang et al., 2015). This relationship allows methane clumped isotope abundances to be used as a geothermometer to constrain gas formation temperatures (Stolper et al., 2014b, Wang et al., 2015). The temperature dependence of clumped-isotope abundances is not unique to methane and exists for all studied materials including CO_2 (Eiler and Schauble, 2004), carbonate-bearing minerals (Ghosh et al., 2006), O_2 (Yeung et al., 2012), and N_2O (Magyar et al., 2016). Clumped isotope abundance in systems that are not in internal isotopic equilibrium can also be used to provide constraints on non-equilibrium processes including the chemical kineticsof various reactions, which we discuss here as well (Daëron et al., 2011, Saenger et al., 2012, Stolper et al., 2015, Wang et al., 2015, Yeung et al., 2015).

In this review, we present a new and substantially expanded database of clumped isotope compositions for methane from a diverse set of formation environments, and discuss the implications of these new data alongside previously published datasets (Ono et al., 2014, Stolper et al., 2014a, Stolper et al., 2014b, Inagaki et al., 2015, Stolper et al., 2015, Wang et al., 2015, Douglas et al., 2016, Young et al., 2017). The purpose of this review is to explore the potential of clumped isotopes to decipher methane origins. We begin with a brief overview of the two different measurement techniques currently available. We then discuss the different processes that control methane clumped isotope values. Finally, we review the broad patterns of clumped isotope abundance in methane from different environments, compare these data with conventional isotope and gas composition

measurements, and discuss potential applications involving the atmosphere and the surface of other planets.

2. Analytical methodology

2.1. Measurement techniques for methane clumped isotope analysis

Two distinct measurement techniques were developed over the past five years for methaneclumped isotope analysis. The first employs high-resolution dual-inlet mass spectrometerswith an electron ionization source. The first such instrument developed was the Thermo MAT-253 Ultra (hereafter referred to as the 'Ultra'), described in detail by Eiler et al. (2013). Methane clumped isotope compositions measured by the prototype version of the Ultra combine the abundances of the two mass-18 isotopologues of methane ($^{13}CH_3D$ and $^{12}CH_2D_2$), but distinguish the two mass-17 isotopologues ($^{13}CH_4$ and $^{12}CH_3D$) (Stolper et al., 2014a). Given the low natural abundance of D, the combined mass-18 ion current is primarily (~98%) determined by the abundance of $^{13}CH_3D$ (Stolper et al., 2014a). More recently, a prototype version of a larger-radius high-resolution isotope ratio mass spectrometer, the Nu Instruments Panorama, that can routinely resolve $^{13}CH_3D$ and $^{12}CH_2D_2$ was developed (Young et al., 2016, Young et al., 2017). A newer, production version of the Thermo Ultra employs an improved beam-focusing and detection design that also allows it to resolve the two mass-18 isotopologues (Clog et al., 2015).

The other measurement technique employs long path-length laser spectroscopy using mid-infrared frequencies. Spectroscopic measurements of methane clumped isotopes were first performed using a difference-frequency-generation laser (Tsuji et al., 2012), but this technique gave relatively poor precision (~20‰). More recently, Ono et al. (2014) developed a tunable infrared laser direct absorption spectroscopy (TILDAS) method that can measure $^{13}CH_3D$ abundance with greatly improved precision (~0.25‰). This technique uses two quantum cascade lasers tuned to four different isotopologues of methane ($^{12}CH_4$, $^{13}CH4$, $^{12}CH_3D$, and $^{13}CH_3D$). Measurement of $^{12}CH_2D_2$ is not currently possible with production version laser spectroscopy systems, but is possible in principle and may be developed in the future. In addition, development of cavity ringdown spectroscopy for methane isotopologues, including clumped isotope species, is ongoing (Bui et al., 2014). The sensitivity and precision of the mass spectrometric and spectroscopic methods for methane clumped isotope analyses are broadly similar. Inter-calibration of these two measurement techniques has not yet been performed, and is a key priority for future research.

2.2. Nomenclature

Conventional carbon and hydrogen isotopic compositions are expressed using delta notation relative to standard mean ocean water (VSMOW) and Pee Dee Belemnite (VPDB), respectively:

$$\delta D = \left(\frac{^{2}R_{sample} - ^{2}R_{VSMOW}}{^{2}R_{VSMOW}} \right) \quad (1)$$

$$\delta^{13}C = \left(\frac{^{13}R_{sample} - ^{13}R_{VPDB}}{^{13}R_{VPDB}} \right) \quad (2)$$

where ^{2}R and ^{13}R are the ratios D/H and $^{13}C/^{12}C$ respectively. Delta values are commonly expressed as per mil (‰) values, which implicitly includes a multiplicative factor of 1000 (Coplen, 2011).

All of the previously unpublished clumped isotope data presented in this paper are combined measurements of the two mass-18 isotopologues performed using the prototype Ultra, and are expressed using Δ_{18} notation (Stolper et al., 2014a):

$$\Delta_{18} = \left(\frac{^{18}R}{^{18}R^{*}} \right) - 1 \quad (3)$$

where:

$$^{18}R = \frac{([^{13}CH_3D] + [^{12}CH_2D_2])}{[^{12}CH_4]} \quad (4)$$

The specified isotope ratios are measured from the corresponding ion beam current ratios, and are standardized by comparison with a gas of known isotopic composition. $^{18}R^{*}$ is the ratio expected for a random distribution of isotopes among all isotopologues, and is calculated using the measured ^{13}R and ^{2}R values for the sample (Stolper et al., 2014a):

$$^{18}R^{*} = (6 \times^{2} R^{2}) + (4 \times^{2} R \times^{13} R) \quad (5)$$

The prefactors 6 and 4 in Eq. (5) derive from the symmetry numbers of the mass-18 methane isotopologues (Stolper et al., 2014a). Δ_{18} values are reported as per mil (‰) deviations from a calculated reference frame, where 0‰ represents a random distribution of methane isotopologues (i.e., $^{18}R = {}^{18}R^{*}$) – this is equivalent to the Δ_{18} value of a gas internally equilibrated at infinite temperature. As gases cannot, in practice, be equilibrated at infinite temperature, all samples are calibrated against a laboratory standard with a Δ_{18}value of 2.981‰, as described by Stolper et al. (2014a). Most of the new data presented in this paper were measured during a period in which we observed a linear dependence of Δ_{18}on ^{18}R in heated gas samples, i.e. the measured state of clumping depends slightly on the level of ^{13}C or D enrichment, which it clearly should not. A correction for this dependence was applied as detailed by Douglas et al. (2016).

We also discuss a smaller subset of previously published data measured using the TILDAS spectroscopy technique or the Nu Panorama mass

spectrometer (about 20% of the total dataset), which are reported as $\Delta^{13}CH_3D$ values, as defined by Ono et al. (2014). We have not converted $\Delta^{13}CH_3D$ values to Δ_{18} values. In the case of methane inferred to have formed in isotopic equilibrium we primarily discuss the data in terms of equivalent temperature (see below), in which case we employ the distinct temperature calibrations for each measurement. In the case of kinetic fractionations, the contribution of $^{12}CH_2D_2$ to Δ_{18} values is uncertain, and therefore an accurate conversion between these measurements is not straightforward. However, we expect that such small differences are unlikely to influence the broad patterns of abundance that we seek to outline here.

Δ_{18} values can be related to equivalent temperature (which has physical meaning as an environmental temperature if the sample has achieved internal isotopic equilibrium), via the equation (Stolper et al., 2014a):

$$\Delta_{18} = -0.0117\left(\frac{10^6}{T^2}\right) + 0.708\left(\frac{10^6}{T^2}\right) - 0.337 \quad (6)$$

The analogous relationship for $\Delta^{13}CH_3D$ is:

$$\Delta^{13}CH_3D = -0.0141\left(\frac{10^6}{T^2}\right) + 0.699\left(\frac{10^6}{T^2}\right) - 0.311 \quad (7)$$

as derived from the calculations of Webb and Miller III (2014). We hereafter refer to such estimated temperatures as T_{18} or T_{13CH3D} values. When referring to both measurements together we refer to Δ_{18} or T_{18}, as this is the more general term.

2.3. Sample preparation

Samples analyzed for this study were prepared using the protocol described by Stolper et al., 2014a, Stolper et al., 2014b. In brief, mixed gas samples were introduced from either a steel cylinder, an aluminum cylinder, or a glass serum vial sealed with a butyl stopper, into a glass vacuum line. Gas samples were first exposed to liquid nitrogen to trap H_2O, CO_2, and H_2S. The gases in the headspace (including CH_4, O_2, and N_2) were then exposed and transferred to a 20 K cold trap, and residual gases, including He and H_2, were pumped away. The cold trap was then sealed, heated to 80 K, cooled to 45 K, and opened to vacuum to remove N_2 and O_2. This temperature cycling was repeated until < 2.67 Pa of gas remained in the cold trap at 45 K, corresponding to a purity of CH_4 of ~99.8% (Stolper et al., 2014a). The cryostat was then heated to 70 K, and CH_4 was transferred to a Pyrex™ breakseal containing molecular sieve (EM Science; type 5A) immersed in liquid N_2. Prior to introduction to the mass spectrometer dual inlet, samples were heated using a heat gun or copper block set to ~150 °C for 2–3 h to ensure minimal isotopic fractionation when transferring CH_4 from the molecular sieves (Stolper et al., 2014a).

2.4. Natural gas reservoir temperature measurements and estimates

For a subset of samples we compared clumped isotope derived temperature estimates with independent measurements or estimates of the natural gas reservoir temperature (see Sections 3.1 Formation or re-equilibration temperature, 4.7 Deep subsurface microbial methane) determined using various methods. Methods for reservoir temperatures for the published Haynesville and Marcellus Shales, Gulf of Mexico, Powder River Basin, Western Pacific, and Birchtree Mine samples were detailed previously. Briefly, temperatures from the Gulf of Mexico are borehole temperatures corrected using proprietary formulas (Stolper et al., 2014b), temperatures from the Haynesville and Marcellus Shale are borehole temperatures with an upwards correction of 10% (Stolper et al., 2014b), temperatures from the Powder River Basin and Birchtree Mine samples were measured in associated formation waters (Bates et al., 2011, Wang et al., 2015, Young et al., 2017), and temperatures from the Western Pacific are estimated from the local geothermal gradient (Inagaki et al., 2015). Shallow marine methane samples from the Santa Monica Basin and the Beaufort Sea (Fig. 2) were compared with measured bottom water temperatures (Stolper et al., 2015, Douglas et al., 2016).

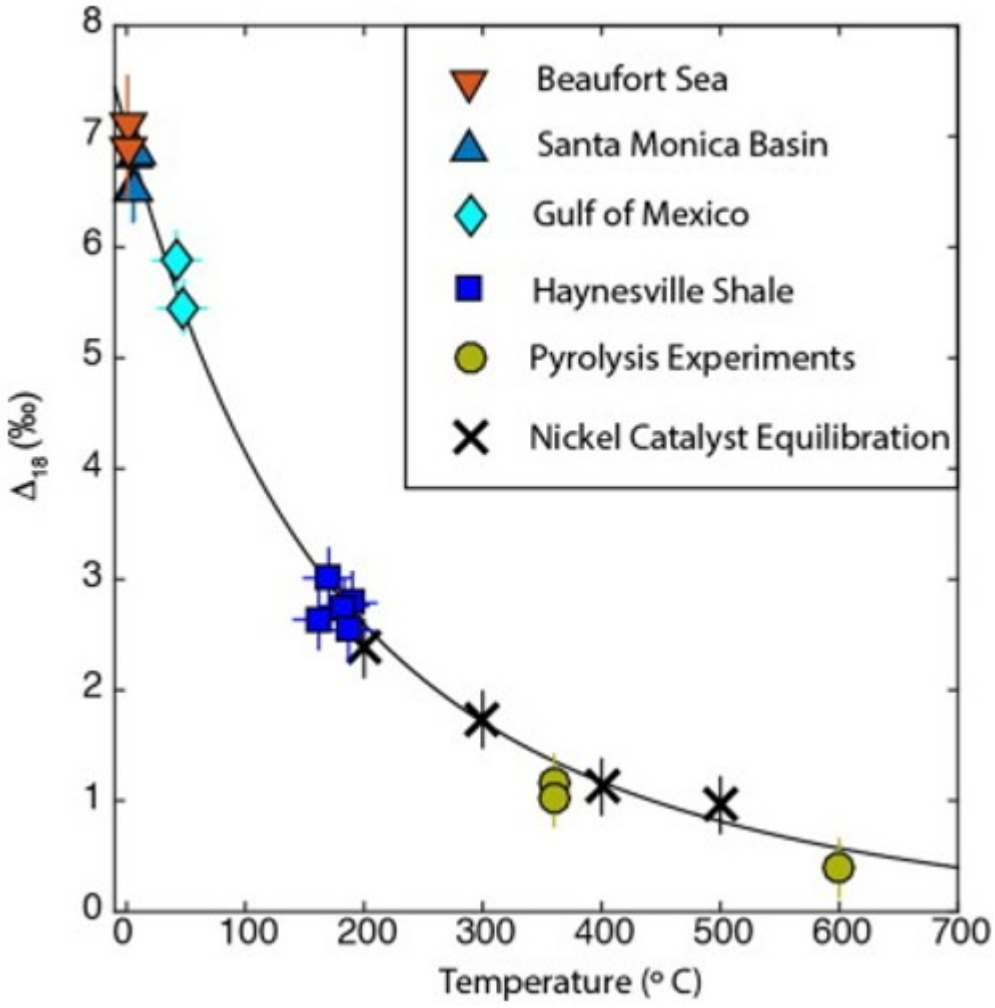

Fig. 2. The relationship between Δ_{18} values and formation temperature for methane formed in internal isotopic equilibrium. The black line indicates the theoretical prediction (Stolper et al., 2014a). The data depicted are either naturally occurring methane with well-constrained formation temperatures (See Section 2.4), or experimentally derived methane (Stolper et al., 2014a, Stolper et al., 2014b, Stolper et al., 2015, Douglas et al., 2016). A similar relationship exists for $\Delta^{13}CH_3D$ values (Ono et al., 2014, Webb and Miller, 2014, Wang et al., 2015). 20 °C error bars in formation temperature were applied to the Gulf of Mexico and Haynesville Shale samples, whereas x-axis errors for other data are smaller than the markers.

Reservoir temperature measurements for the Qaidam and Songliao Basins (Supplementary Table) were based on long-term drill-stem tests, which is a robust method for determining virgin formation temperatures (Hermanrud et al., 1991, Peters and Nelson, 2012). Reservoir temperature estimates for the Milk River Formation (Supplementary Table) were calculated using the local geothermal gradient (estimated using a basin model), the surface temperature, and the depth of the sampled well. An example of this methodology is provided by Nunn (2012). Aside from drill-stem tests, the methods used for reservoir temperature estimation are approximate, and their uncertainties are not consistently quantified. Therefore we applied a conservative 20 °C error to these estimates (Peters and Nelson, 2012; see Sections 3.1 Formation or re-equilibration temperature, 4.7 Deep subsurface microbial methane). For temperatures derived from drill-stem tests we applied a 10% error.

3. Processes Controlling Methane Clumped Isotope Values

3.1. Formation or re-equilibration temperature

Δ_{18} or $\Delta^{13}CH_3D$ values of methane in internal isotopic equilibrium are predicted to vary as monotonic functions of the temperature of equilibration (Fig. 2), as described by Eqs. (6), (7)above (Stolper et al., 2014a, Webb and Miller, 2014, Wang et al., 2015). In most environments internal isotopic equilibrium is not dependent on isotopic exchange between methane molecules, but instead is produced via isotope-exchange reactions with other phases, including H_2O, H_2, or CO_2. However, it is not necessary for methane to be in carbon or hydrogen isotope equilibrium with co-occurring molecules to achieve internal isotopic equilibrium, as long as hydrogen isotope exchange reactions between methane and other molecules are reversible, allowing the distribution of isotopes in C-H bonds in methane to reach equilibrium. For more detailed discussions of the theory of equilibrium clumped isotope fractionation see Wang et al., 2004, Eiler, 2007, Eiler et al., 2014, Stolper et al., 2014a, Wang et al., 2015, Young et al., 2017, Stolper et al., in press.

The clumped isotope temperature dependence for methane formed in isotopic equilibrium is grounded in statistical thermodynamics (Ono et al., 2014, Stolper et al., 2014a, Webb and Miller, 2014, Wang et al., 2015, Young et al., 2017) and has been empirically validated using various methane samples having known equilibration or formation temperatures (Fig. 2). These include methane equilibrated using a metal catalyst (e.g., Ni or Pt) at temperatures between 150 and 500 °C (Ono et al., 2014, Stolper et al.,

2014a, Wang et al., 2015, Douglas et al., 2016); methane from pyrolysis experiments performed at 360 and 600 °C (Stolper et al., 2014b); and methane from environmental samples inferred to have formed in isotopic equilibrium and with independently constrained formation temperatures (Stolper et al., 2014b, Stolper et al., 2015, Douglas et al., 2016). Additional measurements of samples generated between ~50 and 150 °C would improve the Δ_{18}-temperature calibration.

The environmental samples shown in Fig. 2 are all from contexts where methane formed at or near the sampling environment, and where significant migration of gas from other environments is unlikely (Stolper et al., 2014b, Stolper et al., 2015, Douglas et al., 2016). For example, the Haynesville Shale is considered to be both the source and the reservoir for generated hydrocarbons, and its current temperature is within 17 °C of modeled maximum burial temperatures (Curtis, 2002, Stolper et al., 2014b).

Δ_{18} values vary as a non-linear function of temperature (Fig. 2), and the typical precision of Δ_{18} measurements (~0.25‰; 1σ) corresponds to varying temperature errors. For example,±0.25‰ corresponds to an uncertainty of ±8 °C at an inferred temperature of 25 °C, whereas at an inferred temperature of 200 °C the corresponding uncertainty is ±21 °C.

The formation or re-equilibration of methane in internal isotopic equilibrium, whether in the laboratory or environment, requires processes that allow the C-H bonds in methane to reversibly exchange. In a laboratory setting, nickel or platinum catalysts have been used to equilibrate methane C-H bonds at temperatures from 150 to 500 °C over a period of one to two days (Ono et al., 2014, Stolper et al., 2014a, Wang et al., 2015, Douglas et al., 2016). Methane from the Marcellus Shale with a measured well temperature of 60 ± 10 °C (See Section 2.4) yields a T_{18} value of ~200 °C, which is generally consistent with inferred formation conditions. This suggests that methane formed at a higher temperature in isotopic equilibrium, consistent with modeled maximum burial temperatures, and was subsequently uplifted and stored for millions of years at lower temperatures without experiencing re-equilibration (Stolper et al., 2014b). This suggests that internal re-equilibration of methane either does not occur, or proceeds very slowly, at temperatures below 200 °C in shale reservoirs in the absence of significant amounts of metal catalysts.

Internal isotopic equilibrium of methane in natural environments may depend on factors other than storage temperature. For example, H-exchange rates (the main process driving equilibration) may be enhanced by the presence of certain clay minerals or other ‘natural catalysts’ (Alexander et al., 1982, Alexander et al., 1984, Horita, 2001). It has been argued that enzymatic catalysis during anaerobic oxidation of methane by marine archaea induces carbon isotope equilibrium between CH_4 and CO_2 (Yoshinaga et al., 2014), and this process might also induce CH_4 clumped isotope equilibrium (Stolper et al., 2015).

Conventional (δD and $\delta^{13}C$) isotope values in thermogenic methane are generally thought to be controlled by kinetic isotope effects, as opposed to equilibrium fractionation (e.g. Sackett, 1978, Tang et al., 2000, Ni et al., 2011). However, the inference of clumped isotope equilibrium in thermogenic methane is not inconsistent with kinetic isotope effects controlling its $\delta^{13}C$ or δD values (Stolper et al., in press). This is because it is not necessary for methane to fully equilibrate with an external carbon or hydrogen-bearing phase in order for reversible isotope exchange reactions to equilibrate the distribution of isotopes within the C-H bonds of methane. Evidence for clumped isotope equilibrium in both pyrolysis experiments and natural gas samples has been found in several studies (Stolper et al., 2014b, Wang et al., 2015, Young et al., 2017), including consistent results from the measurement of two multiply substituted isotopologues ($^{13}CH_3D$ and $^{12}CH_2D_2$; Young et al., 2017). As discussed in the following section, some recent pyrolysis experiments have yielded clumped isotope results indicating distinctive kinetic fractionations, in which case the T_{18} value is much higher than the experimental temperature (Shuai et al., in revision). Additional experimental and theoretical studies are needed to better understand the mechanisms for developing clumped isotope equilibrium in thermogenic methane, and how this relates to $\delta^{13}C$ and δD values (see detailed discussion in Stolper et al., in press).

3.2. Kinetic isotope effects during methane generation

Methane produced by methanogens in a number of pure culture experiments is characterized by clumped isotope values significantly lower (−5.4 to 2.3‰; Fig. 3) than would be expected based on the experimental temperatures. Such ‘low’ Δ_{18} and $\Delta^{13}CH_3D$ values correspond to apparent formation temperatures that are either significantly higher (216–620 °C) than those of the actual growth temperatures (25–85 °C), or, in the case of negative Δ_{18} values, do not correspond to any possible formation temperature (Fig. 2) (Stolper et al., 2014b, Stolper et al., 2015, Wang et al., 2015, Douglas et al., 2016, Young et al., 2017). Similarly, microbial methane sampled from freshwater ecosystems, cow rumen,
and serpentinization zones also yields either negative clumped isotope values or values that are so low that they cannot plausibly be interpreted as formation temperatures (Stolper et al., 2015, Wang et al., 2015, Douglas et al., 2016) (Fig. 3). These studies hypothesized that the low observed clumped isotope values are the result of kinetic isotope effects arising during microbial methane generation. Specifically, these studies proposed that the low Δ values (either Δ_{18} or $\Delta^{13}CH_3D$) result from the expression of kinetic isotope effects during irreversible, enzymatically-catalyzed hydrogenation of C from CO_2 or CH_3 groups. It has been hypothesized that the degree of enzymatic reversibility dictates how low the Δ value will be, with the least amount of reversibility being linked to the lowest Δ values. We refer to this as the ‘reversibility of methanogenesis’ hypothesis, which is based on and consistent with earlier work relating D/H and $^{13}C/^{12}C$ isotope fractionation in

microbial methanogenesisto the chemical potential gradient between the reactants, such as H_2, CO_2, or methyl groups, and products (CH_4) of methanogenesis (Valentine et al., 2004, Penning et al., 2005).

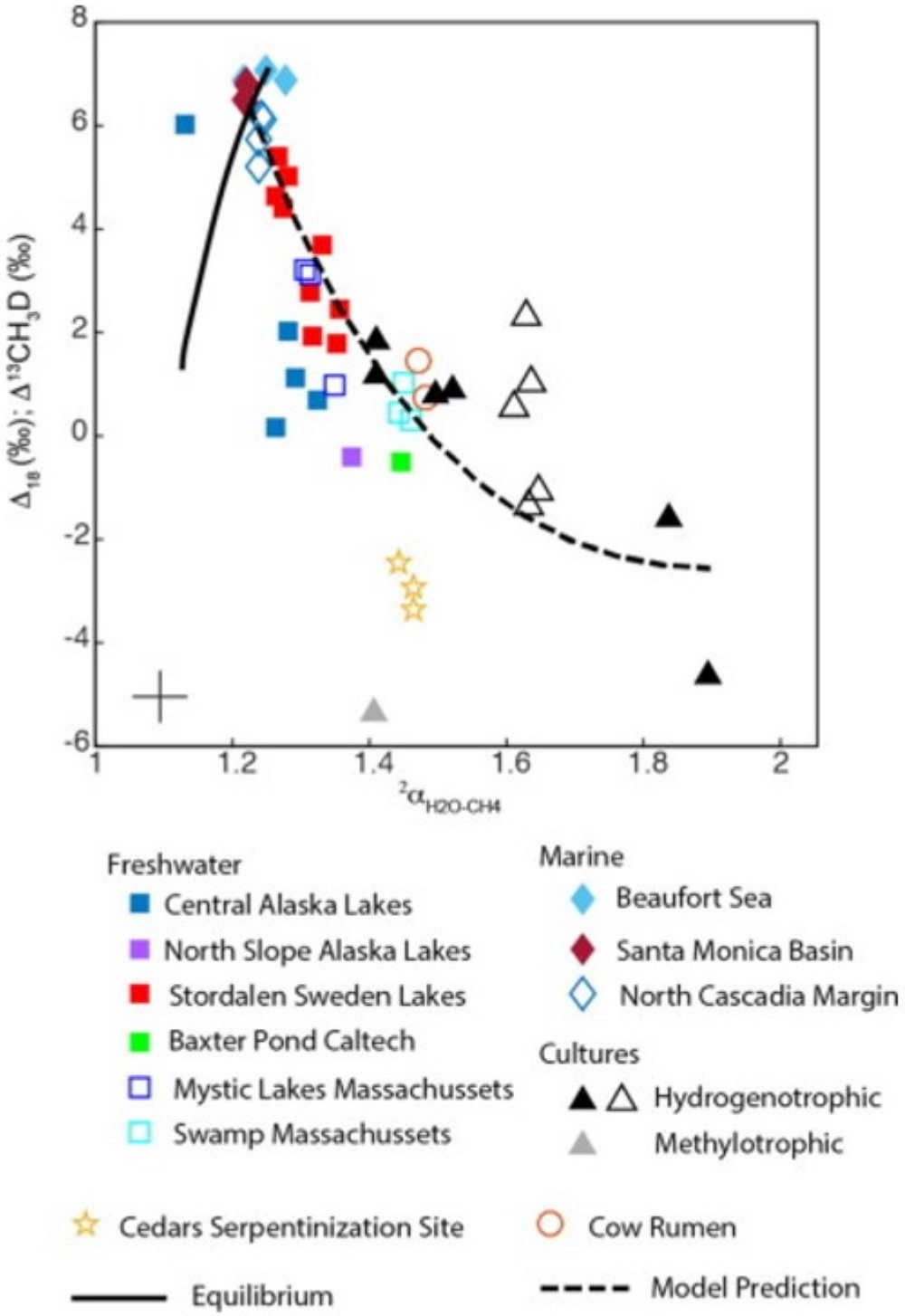

Fig. 3. Plot of clumped isotopes values (Δ_{18} or $\Delta^{13}CH_3D$) vs. $\alpha_{H2O-CH4}$ for microbial methane samples. Deep subsurface microbial methane samples are not plotted since δD_{H2O} values are uncertain. Equilibrium values for Δ_{18}*vs.* $\alpha_{H2O-CH4}$, as calculated by Stolper et al. (2015) are shown by the solid black

line. Samples analyzed for Δ_{18} values are shown by solid markers, whereas samples analyzed for $\Delta^{13}CH_3D$ values are shown by open markers. The samples are categorized by environment and geographic region. Marine microbial methane samples plot near the equilibrium line, but samples from other categories exhibit a negative trend with lower clumped isotope values and higher $\alpha_{H2O\text{-}CH4}$ values than the equilibrium line. The dashed line indicates the predicted trend for decreasing enzymatic reversibility of methanogenesis at 20 °C based on a model of kinetic isotopic effects (Stolper et al., 2015). For freshwater microbial methane there appear to be differences in this trend in different geographic regions. A single pure culture of a fermentative methanogen clearly deviates from the model prediction, with a low Δ_{18} value relative to its $\alpha_{H2O\text{-}CH4}$ value. The cross in the lower left indicates representative x and y error bars. Data from Stolper et al., 2015, Wang et al., 2015, Douglas et al., 2016.

A clear relationship emerges for microbial methane in which Δ_{18} values correlate with $\alpha_{H2O\text{-}CH4}$ (i.e., the hydrogen isotope fractionation between methane and water; Fig. 3). This relationship indicates that the same processes controlling the Δ_{18} values also set the δD value of methane relative to the source water. Importantly, when Δ_{18} values indicate formation temperatures consistent with the environmental temperatures of methanogenesis (Δ_{18} of 5.5–7, corresponding to temperatures between 50 and 0 °C), the $\alpha_{H2O\text{-}CH4}$values are also usually consistent with formation in isotopic equilibrium at that temperature (Fig. 3). Based on this, quantitative models have been created that relate the reversibility of methanogenesis to both the bulk isotopic compositions of microbial methane ($\delta^{13}C$ and δD) as well as Δ_{18} values (Fig. 3). These models are capable of describing, to first order, the co-variation between $\alpha_{CH4\text{-}H2O}$ values and Δ_{18} values (Stolper et al., 2015, Wang et al., 2015). However, the models applied thus far have multiple free parameters and do not supply unique solutions. In any case, the agreement of these models with available data from pure cultures and natural microbial methane samples indicates that they are useful descriptions of the key processes that control the microbial formation of methane (Fig. 3).

These models were developed to characterize fractionations in hydrogenotrophic methanogenesis. To date, there have been two published analyses of fermentative (specifically methylotrophic) methanogenesis from a pure culture (Douglas et al., 2016, Young et al., 2017), only one of which published the δD value of the culture media water. The result from that study deviates significantly from the model predictions, with low Δ_{18}relative to $\alpha_{CH4\text{-}H20}$ (Douglas et al., 2016) (Fig. 3). Possible explanations for this deviation are discussed in detail by Douglas et al. (2016). One plausible explanation is that fermentative methane derives a portion of its hydrogen atoms (50–75%) from methyl groups (Pine and Barker, 1956, Waldron et al., 1999), and therefore may not express $\alpha_{CH4\text{-}H20}$values as large as those expressed by hydrogenotrophic methanogenesis, which derives all of its hydrogen atoms from H_2 in isotopic equilibrium with water (Daniels et al., 1980, Valentine et al., 2004). Indeed, correcting for this effect in methylotrophic methanogenesis experiments leads to $\alpha_{CH4\text{-}H20}$ values that more closely agree with the model predictions (Fig. 8 in Douglas et al., 2016). Some methane samples obtained from freshwater and serpentinization environments also deviate from the model prediction

similarly to the methylotrophic methane, although to a lesser degree (Fig. 3). This is consistent with the observation that fermentative methanogenesis occurs widely in freshwater environments(Ferry, 1993, Borrel et al., 2011).

To first order, the ‘reversibility of methanogenesis’ hypothesis predicts that faster rates of methanogenesis (per cell), stimulated by larger chemical potential gradients between methane precursors and methane, will lead to lower Δ_{18} values. While it is unclear to what extent other environmental or biological variables modulate this relationship, it is possible that Δ_{18} values could serve as an indicator of specific growth rate of methanogens (Stolper et al., 2015, Wang et al., 2015). Such a proxy could improve understanding of the biogeochemistry and ecology of microbial methanogenesis in different environments.

There are also preliminary indications that kinetic isotope effects can be induced in high-temperature catagenetic reactions, at least in the laboratory. While early hydrous pyrolysis experiments performed with shale samples produced Δ_{18} values that were within error of the predicted equilibrium value for the experimental temperature (Fig. 2) (Stolper et al., 2014b), more recent experiments performed with coals at faster heating rates have yielded Δ_{18}values lower than predicted for equilibrium, and in some cases negative ‘anti-clumped’ values (Shuai et al., in revision). While mechanisms for these deviations remain incompletely understood, Shuai et al. (in revision) hypothesize that the observed non-equilibriumfractionation is a result of breaking carbon-carbon bonds during cracking of aliphatic hydrocarbons, whereas demethylation of kerogen produces methane with equilibrium Δ_{18}values. Regardless of the mechanism, it is clear that under some experimental conditions thermogenic methane can be generated that does not form in internal isotopic equilibrium. While most naturally occurring thermogenic methane samples have T_{18} values that are consistent with plausible formation temperatures, kinetic isotope effects may help to explain some cases where T_{18} values appear to be too high, as discussed below (Section 4.5.1).

Recent experiments generating methane via Sabatier reactions using ruthenium catalyst also resulted in strong kinetic isotope effects, as indicated by large negative deviations in $\Delta^{12}CH_2D_2$ and smaller deviations in $\Delta^{13}CH_3D$ relative to the experimental temperature (Young et al., 2017). The authors of this study proposed that the mechanism responsible for kinetic isotope effects observed in these experiments, and possibly in microbial methane as well, involves quantum tunneling effects associated with hydrogen isotope fractionation.

3.3. Mixing effects

As with clumped isotope values for other gases, mixing between end-members that differ in their conventional isotope values (i.e., δD, $\delta^{13}C$) can show non-linear variation in Δ_{18} and $\Delta^{13}CH_3D$ values. This non-linearity results from the definition of Δ_{18} and $\Delta^{13}CH_3D$ values in reference to the stochastic

distribution of mass-18 isotopologues, which is a non-linear polynomial function of δD and $\delta^{13}C$ values (Eq. (5); Fig. 4). The non-linearity of mixing in $\Delta_{18}$is negligible when end-member δD and $\delta^{13}C$ values are similar, but becomes progressively larger as end-member δD and $\delta^{13}C$ values become more widely spaced. Depending on differences in bulk composition, the resultant Δ_{18} values can be either larger or smaller than the expected value for conservative mixing of Δ_{18}. The curvature induced in Δ_{18} by mixing of end-members for two-component mixing is diagnostic of the mixing process (Douglas et al., 2016).

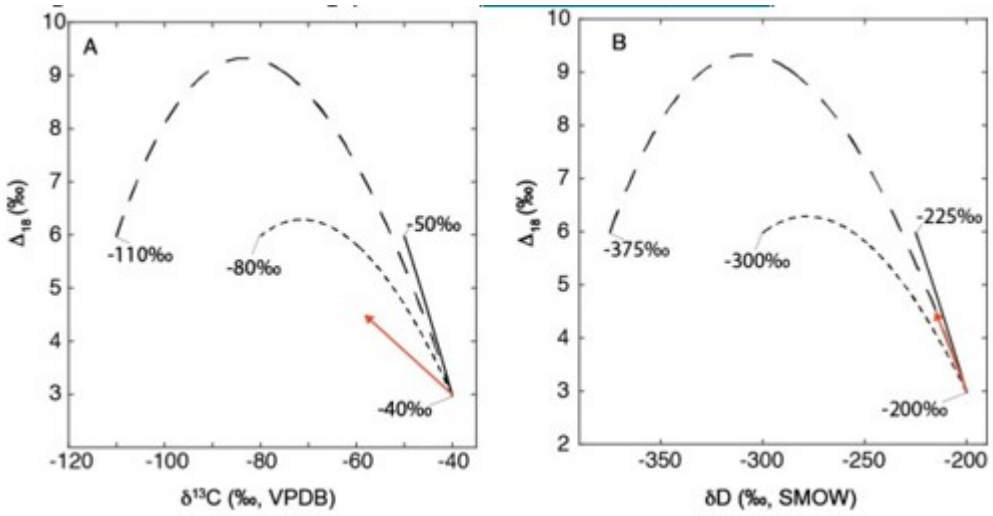

Fig. 4. Hypothetical examples of mixing and diffusion effects for Δ_{18} values, adapted from Douglas et al. (2016). Plots show mixing relationships in $\delta^{13}C$-Δ_{18} space (A) and δD-Δ_{18} space (B) for mixtures of methane with varying end-member compositions. In the mixing examples (black lines) the end-member Δ_{18} values remain fixed, but the end-member $\delta^{13}C$ and δD values vary. For mixtures where $\delta^{13}C$ and δD values are relatively similar, mixing in Δ_{18} is essentially linear (solid line); as the $\delta^{13}C$ and δD values of the mixing end-members become increasingly widely spaced the non-linearity of mixing in Δ_{18} becomes more pronounced (dashed lines). Trajectories for gas-phase interdiffusion of methane in air are shown by the red arrows; the arrow shows the direction of isotopic fractionation of the escaping methane.

The Δ_{18} of some mixed methane samples does not correspond to meaningful formation temperatures (Douglas et al., 2016). However, in some cases the non-linearity of mixing can lead to Δ_{18} values that provide a diagnostic fingerprint of mixing (Fig. 4). If multiple samples of varying mixing ratio can be measured, the calculation of a Δ_{18} mixing curve can provide useful constraints on the isotopic compositions, and potentially formation temperatures, of the mixing end-members (Stolper et al., 2015, Douglas et al., 2016). Alternatively, if the mixtures have similar δD or $\delta^{13}C$ values, the inferred temperature of the mixture will reflect a pseudo-average of the end member Δ_{18} temperatures (Stolper et al., 2014b, Stolper et al., 2015).

3.4. Other kinetic isotope effects

In addition to equilibrium temperature effects, kinetic effects associated with methane generation, and mixing effects, a number of other processes could also have significant effects on Δ_{18} values. Diffusion of methane in either a

vacuum (i.e., gases following Graham's law of diffusion) or diffusion at significant gas pressures in which interactions between particles takes place (i.e., gas-phase interdiffusion) is predicted to increase Δ_{18}values of the gas that escapes relative to the residual, but to decrease δD and $\delta^{13}C$ values of the escaping gas (Fig. 4). Specifically, diffusion of methane through air is predicted to increase Δ_{18} in the escaping gas by 1.5‰, and to decrease δD and $\delta^{13}C$ values in the escaping gas by −19‰. Diffusion through a liquid or solid has unknown effects on Δ_{18}. Similar diffusive fractionations have been described for multiply-substituted isotopologues of CO_2 (Eiler and Schauble, 2004), O_2 (Yeung et al., 2012), and N_2O (Magyar et al., 2016). Fractionation during diffusion through a liquid phase, which is an important transport mechanism for methane in aquatic environments, is unknown both theoretically and experimentally. We note that a sample of methane from gas bubbles at Killarney Lake in Alaska presented an anomalously high Δ_{18} value (9.6‰) and a low $\delta^{13}C$ value (−88.76‰) relative to other Alaskan lake samples, a result that is consistent with diffusive fractionation (Douglas et al., 2016).

Aerobic and anaerobic microbial methane oxidation are critical sinks for methane in many environments, especially in surficial marine and terrigenous environments (Valentine and Reeburgh, 2000, Le Mer and Roger, 2001, Gupta et al., 2013). Methane oxidation generally leads to enrichment of both $\delta^{13}C$ and δD in the residual methane (Whiticar et al., 1986, Whiticar, 1999). Recent closed-system batch-culture experiments constrain how $\Delta^{13}CH_3D$ values are affected by aerobic methane oxidation (Wang et al., 2016), with residual methane decreasing in $\Delta^{13}CH_3D$ as aerobic oxidation proceeds, while $\delta^{13}C$ and δD values increase. These results are consistent with a prediction that the fractionation factor for $^{13}CH_3D$ during aerobic methane oxidation is approximated by the product of the $^{13}C/^{12}C$ and D/H fractionation factors. The effect of aerobic methane oxidation on clumped isotopes in open-system natural environments has not been studied, and could be highly dependent on the interaction of oxidation and transport processes (Wang et al., 2016). Anaerobic methane oxidation employs a biochemical pathway that is distinct from aerobic methane oxidation, and some evidence suggests it leads to partial carbon isotope equilibration of residual methane (Holler et al., 2011, Yoshinaga et al., 2014), but the effect of this process on clumped isotope values has not been studied.

Similarly, reactions with OH^-, and to a lesser extent Cl^-, are major sinks for atmospheric methane (Khalil and Rasmussen, 1983, Kirschke et al., 2013). There have been laboratory observations of kinetic isotope effects for reactions between both OH^- and Cl^- with $^{13}CH_3D$ and $^{12}CH_2D_2$ (Gierczak et al., 1997, Feilberg et al., 2005, Joelsson et al., 2014, Joelsson et al., 2015), which are discussed below in Section 5.1.

4. Methane clumped isotope data from environmental samples

4.1. General patterns of isotopic variation in environmental methane

Clumped isotope measurements of ~250 methane samples have been reported to date, including data from this paper, representing diverse Earth environments. Of these, 135 measurements are presented for the first time here. The totality of Δ_{18} and $\Delta^{13}CH_3D$ data span a wide range of values from −5.4‰ (pure culture of a methylotrophic methanogen; Douglas et al., 2016) to 10.1‰ (a natural gas sample from the Songliao Basin in eastern China; this study). The lowest value for an environmental sample is −3.4‰ ($\Delta^{13}CH_3D$), observed in methane from the Cedars serpentinization zone of Central California (Wang et al., 2015).

Plotting the three isotopic parameters (Δ_{18} or $\Delta^{13}CH_3D$, δD, $\delta^{13}C$) for all samples from natural environments (i.e., not laboratory experiments) reveals a broadly triangular distribution (Fig. 5). Samples with the highest Δ_{18} values generally also have the lowest $\delta^{13}C$ values and intermediate δD values. These samples represent primarily marine and ‘deep’ biosphere (i.e., organisms living in buried sedimentary strata) microbial methane, but also include some samples that are inferred to be from mixed sources. There are two broad but distinct trends of data with decreasing Δ_{18} values (Fig. 5). In one, decreasing Δ_{18} values correspond to increasing $\delta^{13}C$ and δD values (solid line in Fig. 5). This sample set includes most of the thermogenic, volcanic and hydrothermal methane, and some samples from serpentinization systems. In general, T_{18} values for these samples indicate plausible methane formation temperatures (Fig. 6), and we infer that this axis of variability primarily corresponds to equilibrium isotope fractionation. However, some of the samples that plot along this trend are influenced by mixing effects.

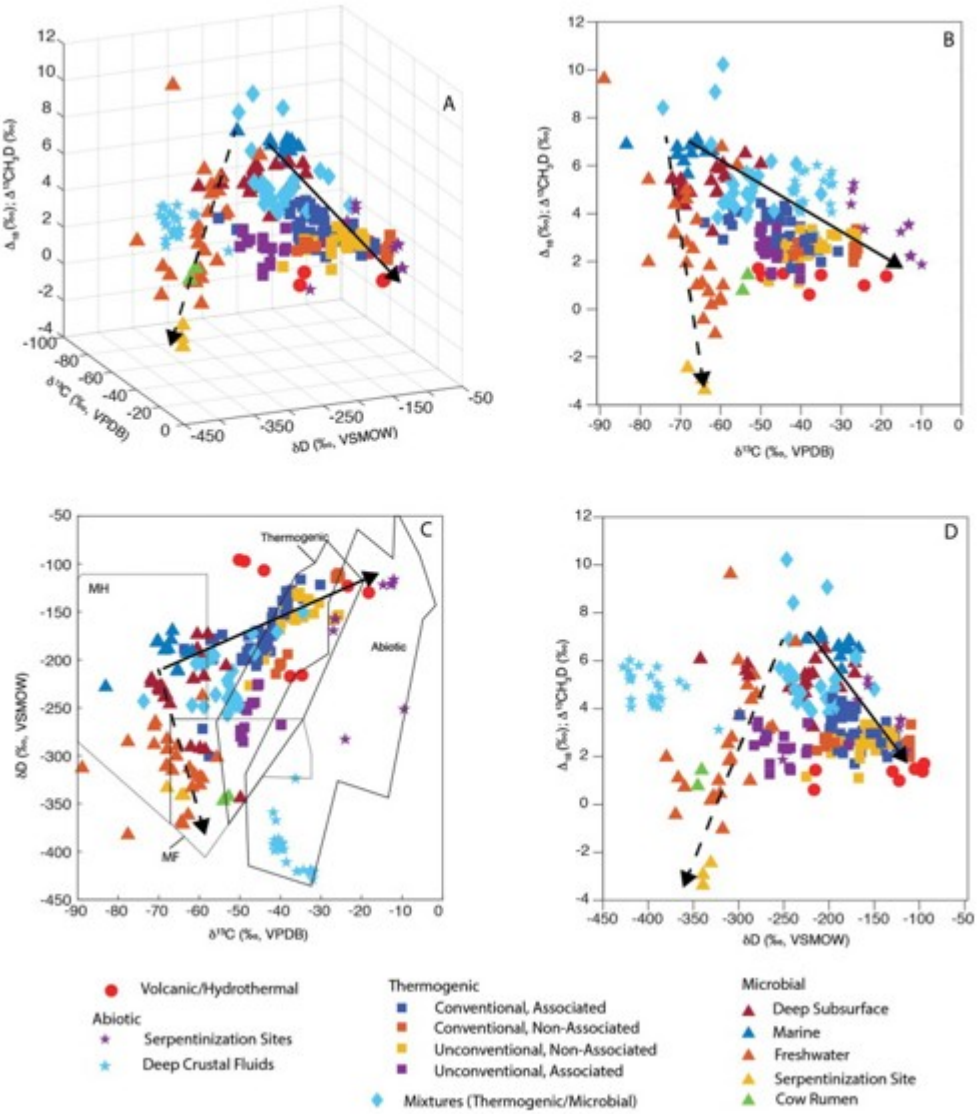

Fig. 5. Plots showing the isotopic distribution of environmental methane (i.e., not produced in laboratory experiments) samples analyzed for clumped isotopes to date. (A) Three-dimensional plot of $\delta^{13}C$ vs. δD vs. clumped isotopes (Δ_{18} or $\Delta^{13}CH_3D$); (B) $\delta^{13}C$ vs. clumped isotopes; (C) δD vs. $\delta^{13}C$; (D) δD vs. clumped isotopes. Empirical fields for different methane sources as defined in Fig. 1 are shown in (C). General trends for equilibrium fractionation (solid line) and kinetic isotope fractionation (dashed line) are indicated in each plot. Data from Stolper et al., 2014b, Inagaki et al., 2015, Stolper et al., 2015, Wang et al., 2015, Douglas et al., 2016, Young et al., 2017 and this study.

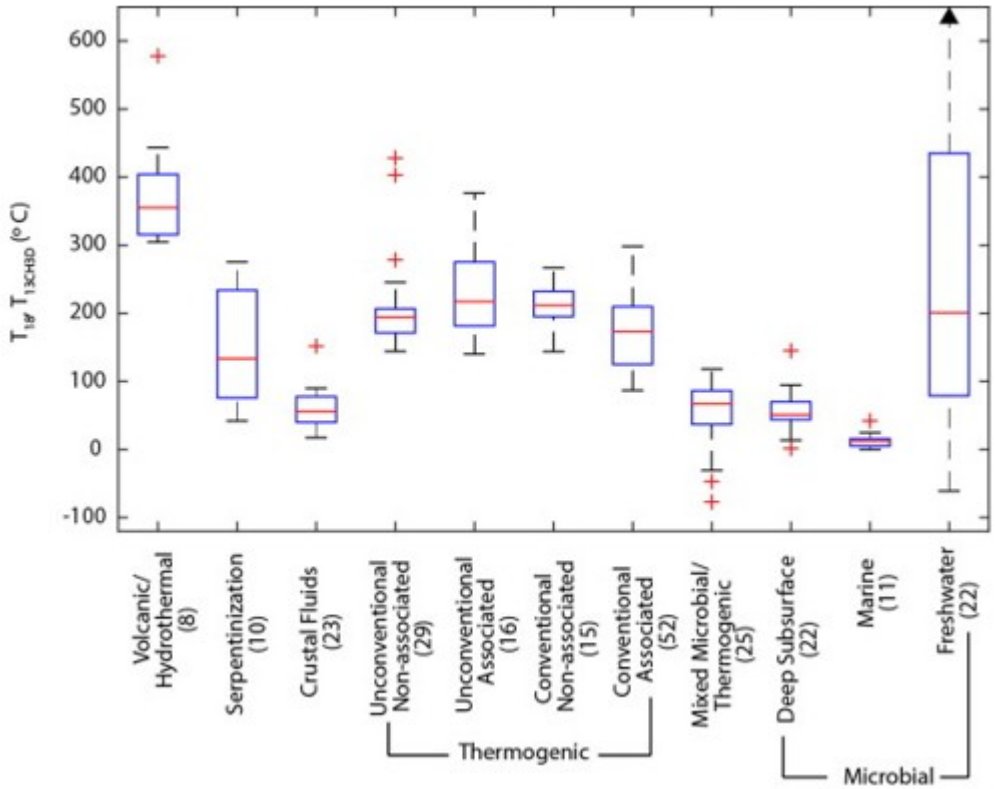

Fig. 6. Plot shows the distribution of formation temperatures inferred from clumped isotope measurements for different categories of environmental methane. The red lines indicate the median value, the blue box indicates the first and third quartiles, the black whiskers indicate the maxima and minima within 1.5 interquartile range of the first and third quartile, and individual points indicate outlier values beyond this limit. The number samples per category is listed. The arrow for freshwater microbial indicates that some values extend beyond 600 °C. Some samples in this category have negative clumped isotope values, which do not correspond to any temperature. Microbial methane samples from serpentinization sites are not shown since these samples have negative $\Delta^{13}CH_3D$ values. Data from Stolper et al., 2014b, Inagaki et al., 2015, Stolper et al., 2015, Wang et al., 2015, Douglas et al., 2016, Young et al., 2017 and this study.

In the other trend, decreasing Δ_{18} values correspond to decreasing δD values, as well as a relatively small increase in $\delta^{13}C$ values (dashed line in Fig. 5). This group of samples include some that yield negative or 'anti-clumped' Δ_{18} or $\Delta^{13}CH_3D$ values. Samples falling along this trend are mainly microbial methane derived from freshwater ecosystems and serpentinization-zone microbial communities and we interpret this trend to represent kinetic isotope effects related to the differential reversibility of microbial methanogenesis, as discussed in Section 3.2.

Some samples do not conform neatly to either of the two isotopic trends discussed above. For example, unconventional oil-associated thermogenic methane samples (See Section 4.4) tend to have lower δD values, relative to their Δ_{18} values, compared to other thermogenic methane samples. Samples from deep crustal fluids (Wang et al., 2015, Young et al., 2017) (see Section 4.4), inferred to be abiotic methane (Sherwood Lollar et al., 2008), have relatively low δD values but high $\delta^{13}C$ values, making them unique in these plots relative to other sample types (Fig. 5).

4.2. Hydrothermal and volcanic methane

Methane emissions from hydrothermal vents and volcanoes are a relatively small component of the global methane budget, contributing about 2–9 Tg/yr (Lacroix, 1993, Etiope et al., 2008), compared to a total global flux of 540–680 Tg/yr (Kirschke et al., 2013). However, methane from these systems can provide important insights into the carbon-cyclegeochemistry of these high-temperature environments. Modern volcanic and hydrothermal methane sources may be an important analogue for the generation of methane on the early Earth, its role in climatic conditions, and the development of life (Emmanuel and Ague, 2007). Methane in volcanic and hydrothermal systems is generally thought to derive from (i) the high-temperature breakdown of buried and/or subducted organic matter (similar to thermogenic methane); (ii) abiogenic synthesis of methane at moderate to high temperatures (~200 to 600 °C); or (iii) mantle-derived methane (Welhan, 1988, Emmanuel and Ague, 2007, Proskurowski et al., 2008). The relative fraction of these sources varies and primarily depends on the amount of sedimentary rocks in the volcanic system (Welhan, 1988). Carbon isotope ratios are often applied to differentiate the source of hydrothermal methane, with high $\delta^{13}C$ values (>−20‰) often interpreted as indicative of abiogenic methane (Welhan, 1988, Fiebig et al., 2015), although experimental and natural data suggest revisions to this interpretive framework (Horita and Berndt, 1999, Etiope and Sherwood Lollar, 2013, Etiope and Schoell, 2014).

There are currently eight CH_4 clumped isotope measurements from hydrothermal and volcanic systems, including four samples from two distinct marine hydrothermal vents, and four from three different terrigenous hydrothermal systems (Supplementary Table). The four samples from marine systems, one from the Guaymas Ridge in the Gulf of California (Wang et al., 2015) and three from the Juan de Fuca Ridge (Supplementary Table), yield formation temperatures from 304 ± 40 to 365 ± 50 °C. These inferred temperatures are within error of vent fluid temperatures, which are estimated at 299 ± 5 °C for the Guaymas Ridge (Reeves et al., 2014), and 324 °C for Bastille and 335 °C for Lobo (maximum measured temperatures) at the Main Endeavour Field on the Juan de Fuca Ridge in July 2014. Methane emitted from Guaymas Ridge was previously interpreted to form from thermocatalysis of buried organic matter (Welhan, 1988), and the low $\delta^{13}C$ values (−44 to −50‰) and relatively high δD values (−96 to −106‰) of all four of these samples are consistent with this mechanism (Fig. 1; Fig. 5). The clumped isotope data suggest that, at least in the studied systems, methane derived from the thermal cracking of organic matter in hydrothermal systems forms at significantly higher temperatures than those commonly observed in natural gas reservoirs (Fig. 6).

The four samples from terrigenous hydrothermal systems indicate generally higher temperatures (364 ± 49 °C at Pantelleria, Italy, 444 ± 79 °C at Nisyros, Greece, 347 ± 45 and 578 ± 109 °C at Washburn Spring,

Yellowstone, USA) (Supplementary Table). It has been suggested that CH_4 and CO_2 at Nisyros and Pantelleria occur in isotopic equilibrium, with carbon isotope fractionation pointing to hydrothermal reservoir temperatures of 320–360 °C and 540 °C, respectively (Fiebig et al., 2004, Fiebig et al., 2013). Accounting for analytical error, the apparent clumped isotopic equilibration temperature for Nisyros is only slightly higher than that determined by Fiebig et al. (2004). Additional clumped isotope data for CH_4 from Nisyros could be used to further evaluate the hypothesis of CH_4 and CO_2occurring in equilibrium. In the case of Pantelleria, the apparent clumped isotopic temperature is significantly lower than that based on the apparent carbon isotope fractionation. This discrepancy either indicates the absence of carbon isotope equilibration between CH_4 and CO_2 in this system, or points to the importance of H-isotope re-equilibration during the ascent of the gases, which could re-set the apparent clumped isotope temperature.

At Washburn Springs in Yellowstone, carbon isotope fractionation between CH_4 and CO_2indicates a formation temperature of 286 °C (Moran et al., 2017), while the temperature of the hydrothermal reservoir is estimated to be 360 °C (Truesdell et al., 1977). One of the clumped isotope analyses indicates a temperature similar to that of the hydrothermal reservoir, while the other is considerably higher. The wide range of inferred temperatures from the Yellowstone samples is intriguing, as it could suggest either differential sources of methane despite similar δD and $\delta^{13}C$ values, or differences in the extent of re-equilibration within the hydrothermal reservoir. However, this difference will need to be validated with further analyses. Overall, the terrigenous hydrothermal data are compatible with high-temperature (> 300 °C) abiotic methane in these systems.

4.3. Methane from low-temperature serpentinization sites

Water–rock interactions in low-temperature terrigenous serpentinization sites (i.e. <150 °C; (Etiope et al., 2011) are also thought to be a source of abiotic methane, with an uncertain global flux (Etiope et al., 2016). The most widely discussed mechanisms for methane production in serpentinization zones are Sabatier or Fischer-Tropsch type reactions in which inorganic carbon (mainly CO_2) combines with molecular hydrogen to form methane (and larger hydrocarbons) and water (Emmanuel and Ague, 2007, McCollom, 2013, Etiope and Schoell, 2014). In many cases, however, it is difficult to rule out contributions of microbial or migrated thermogenic methane in serpentinization zones (Etiope et al., 2011, Etiope et al., 2013).

Clumped-isotope compositions of methane from five different low-temperature serpentinization systems have been analyzed, with widely varying results. These include two sites from central California (Cedars and CROMO), and sites from Turkey (Chimaera), Portugal (Cabeço de Vide), and Italy (Acquasanta). In the Cedars serpentinite site from central California, Wang et al. (2015) observed strongly negative $\Delta^{13}CH_3D$ values (−2.4 to −3.4‰) that clearly indicate non-equilibrium isotope fractionation

during methane generation or migration. These values, alongside low $\delta^{13}C$ (−63.8 to −68.0‰) and δD (−333.1 to −342.0‰) values, were interpreted as indicators of microbial methanogenesis accompanied by strong kinetic isotope effects (Fig. 3). A previous study of the geochemistry of the Cedars serpentinization site suggested that contributions from both abiotic and microbial methane were likely (Morrill et al., 2013), but the clumped isotope data are consistent with a dominantly microbial, strongly non-equilibrium methane source. Interestingly, in a plot of $\Delta^{13}CH_3D$ vs. $\alpha_{H20\text{-}CH4}$, the Cedars samples plot near a sample from a pure culture of fermentative methanogens grown with a methanol substrate (Fig. 3). Morrill et al. (2013)suggested that microbial acetogenesis occurs in these springs, potentially providing a ready source of acetate for fermentative methanogenesis. However, it is currently unknown whether fermentation of methanol versus acetate yields similar clumped isotope compositions.

Methane sampled from wells in the Coast Range Ophiolite Microbial Observatory (CROMO) is significantly more enriched in $\delta^{13}C$ (−26 to −27‰) and δD (−157.5 to −169.5‰) than that at Cedars, and has higher Δ_{13CH3D} values (5.2–4.4‰) consistent with a formation temperature between 42 ± 11 and 76 ± 13 °C (Wang et al., 2015). It remains unclear if the methane sampled from CROMO is abiotic (Wang et al., 2015), but assuming the methane formed in isotopic equilibrium, the inferred temperatures suggest formation within the ophiolite (peridotite) nappe, as generally considered for continental serpentinization sites (Etiope et al., 2016).

Methane emitted at the Chimaera seeps in Turkey (Etiope et al., 2011) is characterized by highly enriched $\delta^{13}C$ (~−12‰) and δD (~−116‰) values that suggest a predominantly abiotic origin. The Δ_{18} values in these samples (2.2–2.3) suggest an equilibrium formation temperature of 235 ± 29 °C (Fig. 6, Supplementary Table). Earlier application of an H_2-CH_4δD geothermometer implied that methane at Chimaera formed at ≤ 50 °C (Etiope et al., 2011), which is clearly at odds with the Δ_{18}-derived temperature. The local geothermal gradient suggests maximum temperatures of 80–100 °C at the base of the ophiolite nappe, within which abiotic methane is considered to have formed (Etiope et al., 2011). It cannot be excluded, however, that methane formed near the metamorphic sole (high-grade metamorphic rocks within the ophiolite complex) during ophiolite obduction, which likely experienced higher temperatures (Etiope et al., 2016). Furthermore, analysis of $\Delta^{13}CH_3D$, both alone and in tandem with $\Delta^{12}CH_2D_2$, indicates methane forming at or near internal isotopic equilibrium at a temperature of 128 ± 10 °C (Wang et al., 2014, Young et al., 2017). The disagreement between the clumped isotope data and the H_2-CH_4 δD geothermometer indicate that the H_2 and CH_4 emitted at the seep are not in isotopic equilibrium.

The difference in inferred temperatures between the different clumped isotope measurements for the Chimaera seep samples is both noteworthy and problematic. We suggest there may be three possible causes for this difference. First, leakage of gas from imperfectly sealed sample containers

could lead to a diffusive isotope effect and a depletion in Δ_{18} in the residual gas, leading to artificially high T_{18} values. Indeed, earlier analyses at Caltech of gas sampled from Chimaera appeared to demonstrate such an effect, with progressively lower Δ_{18} and higher δD and $\delta^{13}C$ values in sample containers with lower methane concentrations. The samples presented here, however, were analyzed later and were stored in better-sealed sample containers. An argument against leakage is the similarity of δD and $\delta^{13}C$ values between samples analyzed at Caltech and at UCLA (Supplementary Table; Young et al., 2017). Second, the difference could reflect unresolved discrepancies in clumped isotope reference frames and standardization between laboratories and methodologies. Third, it is possible, but unlikely, that the difference reflects true isotopic heterogeneity in Chimaera gases. Resolving this difference will require additional interlaboratory calibration and standardization.

Recent coupled analyses of $\Delta^{13}CH_3D$ and $\Delta^{12}CH_2D_2$ indicate that while the Chimaera methane appears to form in isotopic equilibrium, methane at other low-temperature serpentinization sites (Cabeço de Vide, Portugal and Acquasanta, Italy) is not in isotopic equilibrium, and that therefore $\Delta^{13}CH_3D$-derived temperatures from these sites likely do not reflect formation temperatures (Young et al., 2017). The mechanisms for disequilibrium at these sites are not clearly identified, but could reflect kinetic effects induced by surface catalysis, diffusion, and/or mixing effects.

4.4. Deep fracture fluid methane

Methane samples from crustal fluids in Precambrian shield formations from Canada and South Africa were analyzed by Wang et al. (2015) and Young et al. (2017). Methane in these samples was characterized by relatively high $\delta^{13}C$ values between −32 and −42‰, and low δD values between −323 and −421‰ compared to other categories of environmental methane (Fig. 5). $\Delta^{13}CH_3D$ values vary between 3.1 to 6‰, corresponding to temperatures from 25 ± 7 to 150 ± 20 °C. Based on previous observations of methane and higher hydrocarbon isotope values, these samples are believed to be abiotic (Sherwood Lollar et al., 2008). The inferred formation temperatures from Kidd Creek in Canada are generally higher than measured groundwater temperatures (~30 °C) (Sherwood Lollar et al., 2008), but could represent methane that formed deeper in the crust and subsequently migrated to its current thermal environment. However, there is evidence that most of these methane samples formed out of isotopic equilibrium, based both on comparison of $\Delta^{13}CH_3D$ values and $\alpha_{CH4\text{-}H2O}$ values (Wang et al., 2015), as well as comparison of $\Delta^{12}CH_2D_2$ and $\Delta^{13}CH_3D$ values (Young et al., 2017). The proposed mechanisms for disequilibrium in these systems are kinetic isotope effects generated during catalyst-mediated Fischer-Tropsch reactions(Young et al., 2017).

4.5. Thermogenic methane

Thermogenic methane formed by high-temperature breakdown of organic matter in deeply buried sediments (>1 km), is a major component of economically recoverable petroleumsystems. It is also a significant contributor to atmospheric methane, both through natural emissions from seeps and mud volcanoes (50–60 Tg per year) (Etiope et al., 2008, Etiope, 2012, Schwietzke et al., 2016), and through anthropogenic emissions related to fossil fuelextraction, distribution, and use (98–150 Tg per year) (Denman et al., 2007, Schwietzke et al., 2016). We discuss several subcategories of thermogenic methane, primarily defined by the type of reservoir in which the gas is stored. Conventional gas reservoirs generally occur in porous sedimentary rocks capped by an impermeable stratum (Hunt, 1979). Unconventional gas accumulations are generated and reservoired within the source rock, which are typically organic-rich mudrocks (Curtis, 2002, Peters et al., 2015). Unconventional natural gas is typically extracted by hydraulic fracturing of mudrock strata, which releases gas, and in some cases oil. We further subdivide natural gas samples into those that are associated with significant deposits of liquid petroleum ('oil-associated') and those that are not ('non-associated'). Associated gases are either dissolved in oil ('solution gas') or present as a gaseous phase overlying a liquid phase in the reservoir (a 'gas cap'). 'Non-associated' gases are present in the gaseous phase in the reservoir and are not in contact with any liquid hydrocarbons in the subsurface.

Thermogenic natural gas samples comprise by far the largest set of clumped isotope measurements to date, making up approximately 45% of the total dataset. We provide a general overview of patterns observed in these data here, but refer the reader to Stolper et al. (in press) for a more detailed discussion of the application of clumped isotopes in natural gas. In general, thermogenic methane Δ_{18} values indicate formation temperatures from 100 to 300 °C (Fig. 6), which broadly corresponds to estimates of the temperature window for catagenesis of buried organic matter (Quigley and Mackenzie, 1988, Seewald, 2003). A few samples from marine seeps in the Santa Barbara basin, which are believed to be thermogenic in origin, indicate formation temperatures around 90 °C (Supplementary Table), but we cannot rule out a contribution of microbial methane in these samples. There are a number of thermogenic methane samples from unconventional reservoirs with T_{18} estimates greater than 300 °C. These temperatures are higher than expected for catagenetic methane formation in sedimentary basins, and we discuss possible explanations for this discrepancy below (Section 4.5.1).

In general, T_{18} values for methane from oil-associated, conventional reservoirs (mean 171 °C, minimum 87 °C) are lower than those for other thermogenic categories (mean between 205 and 230 °C, and minimum ~140 °C) (Fig. 6). This difference in temperature distributions could be interpreted to mean that methane found in oil-associated conventional reservoirs is often produced via lower temperature cracking of larger organic molecules associated with the 'oil-window' (Quigley and Mackenzie,

1988, Seewald, 2003), whereas other, higher temperature processes (e.g., secondary cracking of larger hydrocarbons produced from kerogen and later stages of kerogen cracking) dominate methane production in the other reservoir categories. However, the upper range of T_{18} values (maximum of 298 °C; Fig. 6) in conventional, oil-associated reservoirs suggests that methane from higher-temperature cracking of shorter-chain hydrocarbons (relative to co-generation of methane with oil) can also be significant in some reservoirs. However, as discussed below (Section 4.5.1), temperatures at the upper range of the T_{18} distribution for all of the categories of thermogenic methane may not reflect accurate formation temperatures, and instead could be influenced by kinetic isotope effects during formation, transport, or extraction.

We observe a weak but significant positive correlation ($R^2 = 0.2$; $p < 0.001$) between $\delta^{13}C$ values and T_{18} estimates for methane in all natural gas reservoirs (Fig. 7A). The trend between $\delta^{13}C$ and T_{18} varies between basins, likely due to differences in the $\delta^{13}C$ value of the source kerogen, among other factors (see Stolper et al., in press for further details). We also observe a weak, but significant, positive correlation between $\delta^{13}C$ and T_{18} in conventional reservoirs ($R^2 = 0.29$; $p < 0.001$). These relationships are consistent with the concept that the $\delta^{13}C$ of methane increases with source rock maturity (Schoell, 1980). However, such a relationship is not observed in unconventional reservoirs, and in fact there is a negative relationship between $\delta^{13}C$ and T_{18} in non-associated, unconventional methane samples ($R^2 = 0.23$, $p < 0.01$). One possible explanation for this negative relationship is that it reflects a non-linear mixing trend between methane formed at different maturities, as described by Stolper et al. (in press). We do not observe a correlation between δD and T_{18}values in any of the thermogenic methane categories (Fig. 7B). Notably, unconventional, associated methane samples generally have lower δD values for a given T_{18} than methane from other types of reservoirs.

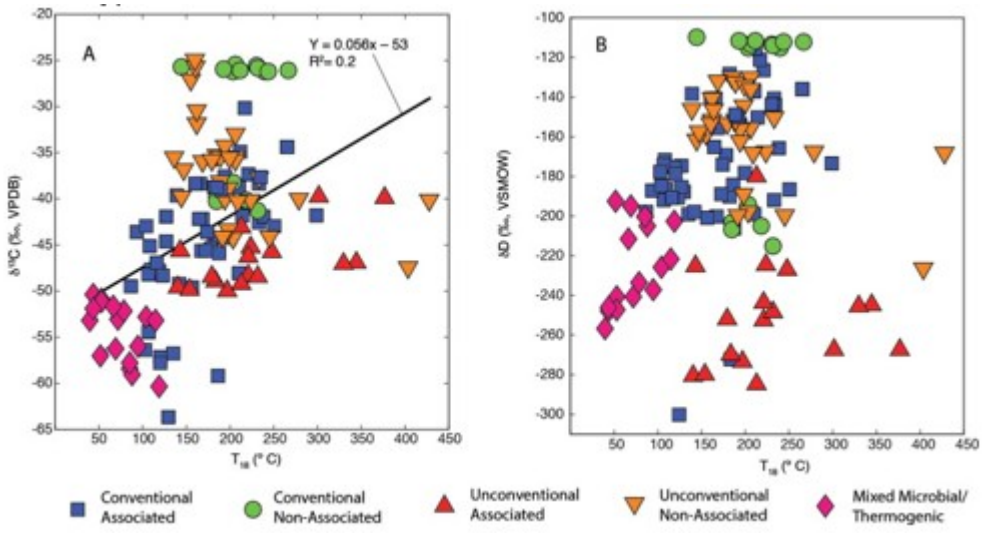

Fig. 7. Plot of (A) $\delta^{13}C$ vs. T_{18} and (B) δD vs. T_{18} values for samples from natural gas reservoirs or seeps. The regression line is fit to the entire dataset depicted. Here we only plot samples of an inferred mixed source from natural gas wells. Data from Stolper et al., 2014b, Stolper et al., 2015, Wang et al., 2015, Young et al., 2017 and this study.

We also compared T_{18} values with ratios of methane to heavier hydrocarbons, i.e., 'gas wetness', calculated here as $[C_1]/[C_2+C_3]$ (Fig. 8). Gas wetness is often used as a qualitative indicator of the maturity of hydrocarbon systems, with higher temperature catagenesis and the associated cracking of smaller hydrocarbons generally producing 'drier', more methane-rich gases (Fig.1B), although initial gases formed at low temperatures are also often relatively 'dry' (Bernard et al., 1978, Hunt, 1979). In our dataset, oil-associated gases (excluding samples from marine hydrocarbon seeps in the Santa Barbara Basin) generally have relatively low $[C_1]/[C_2+C_3]$ values ranging from 1 to 13. This corresponds to a wide range of methane concentrations, from ~50% to ~93%. There is no clear trend in these samples between gas wetness and T_{18}, although interestingly some of the 'wettest' conventional samples have relatively high T_{18} temperatures (>160 °C) that are above the typical oil-window (Hunt, 1979).

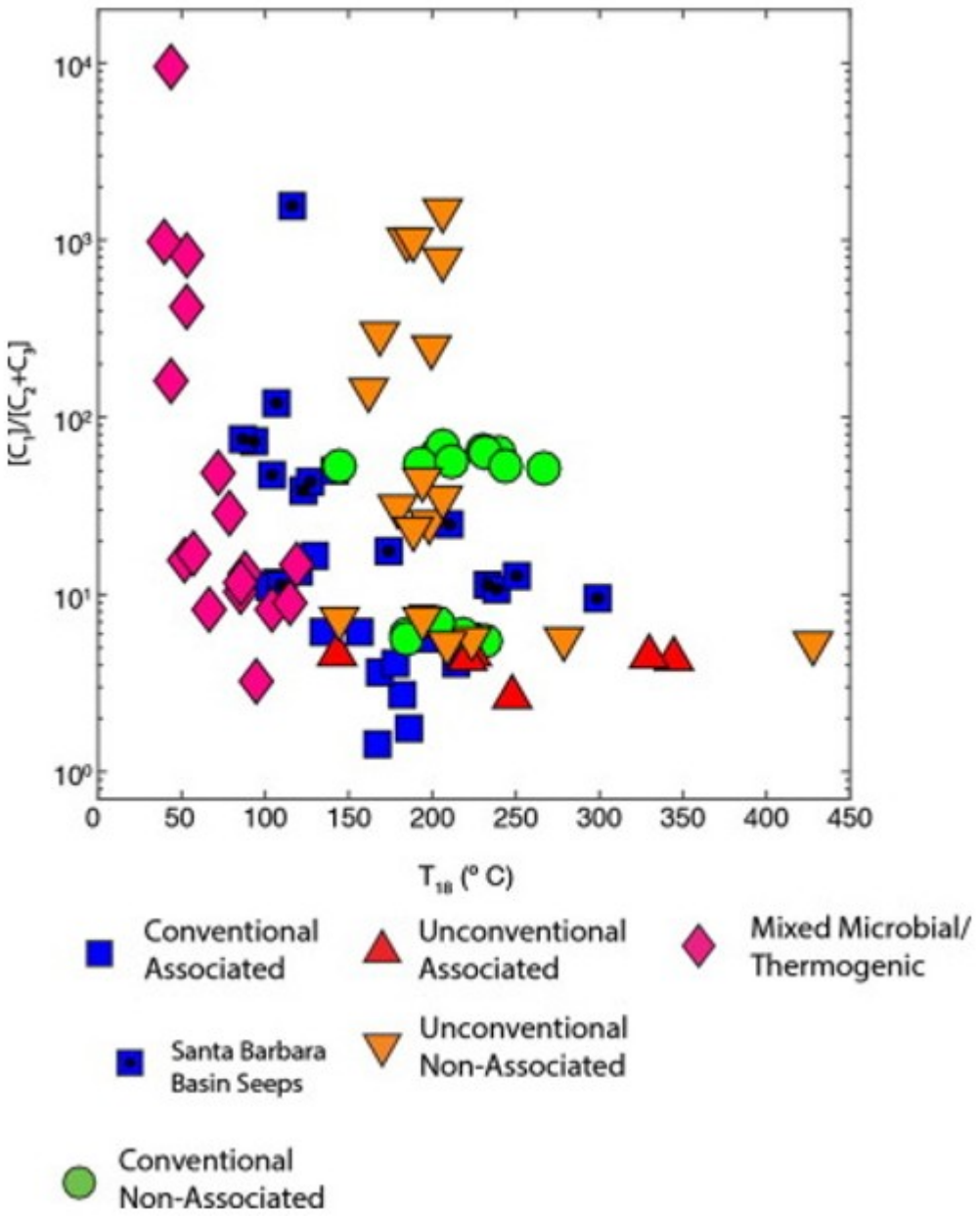

Fig. 8. Plot of $[C_1]/[C_2 + C_3]$ vs. T_{18} values for samples from natural gas reservoirs or seeps. Not all natural gas reservoir samples had gas composition data available. We only plot samples of an inferred mixed source from natural gas wells. Data from Stolper et al., 2014b, Stolper et al., 2015, Wang et al., 2015 and this study.

Gas from hydrocarbon seeps in the Santa Barbara Basin are characterized by higher $[C_1]/[C_2+C_3]$ values for a given T_{18} value than other conventional, oil-associated samples. They also follow a trend similar to that of mixed microbial and thermogenic gases, although with relatively high $[C_1]/[C_2+C_3]$ values. While these gases are generally thought to originate from underlying conventional hydrocarbon reservoirs (Hornafius et al., 1999), this pattern is consistent with molecular fractionation (i.e., an increase in the C1/C2+ ratio during migration) and/or secondary methanogenesis, which are both typical

of many seeps (Etiope et al., 2009). Non-associated gases span a much wider range of $[C_1]/[C_2+C_3]$ values (as high as 10^3), but gas wetness is not clearly related to T_{18} values. Dry gases with $[C_1]/[C_2+C_3]$ greater than ~20 likely represent methane dominantly generated beyond the oil window (>160 °C), which is generally consistent with their T_{18} values.

Methane samples from terrigenous Type-III kerogen in the Rotliegend formation (conventional, non-associated), span a range of T_{18} values from 193 to 267 °C (with the exception of one sample with a lower T_{18} of 144 °C), and a narrow range of $[C_1]/[C_2+C_3]$ values, from 52 to 68. Excluding the outlier, these samples indicate a consistently high formation temperature of 225 ± 26 °C (1σ), which is equivalent to the analytical error at this temperature range. Terrigenous hydrocarbon sources that are older than the Cenozoic, including coal, often generate dominantly dry gas regardless of the thermal maturity of the rock (Schoell, 1983). The T_{18} values in this case indicate dry gas formation from coal source rocks at high temperatures (≥200 °C), although as discussed below (Section 4.5.1) there are several possible factors that could lead to T_{18} values that could be higher than the actual formation temperature. In the case of the Rotliegend Formation the effect of gas diffusionfrom the reservoir or source rock could be important.

4.5.1. Anomalously high T_{18} values in thermogenic methane

In some samples from natural gas reservoirs, T_{18} values indicate formation temperatures that are unrealistically high (Fig. 7, Fig. 8). In some cases these temperatures exceed the nominal upper bound of thermogenic gas generation (~300 °C) (Quigley and Mackenzie, 1988, Seewald, 2003), e.g., in samples from the Eagleford and Bakken shales and the Appalachian Basin.

We suggest four plausible explanations for this phenomenon. First, high apparent clumped-isotope temperatures could be an analytical artifact, either related to sample preparation or analysis. In two samples from the Eagleford Shale that indicated high T_{18} values when prepared using the standard technique, we subsequently re-extracted gas samples while heating the sample cylinder to 85 °C (Fig. 9). This was done because these samples contain non-trivial quantities of C_{4+}hydrocarbons, which would be in the liquid phase at the pressures of the sampled cylinders. The heated extractions yield lower T_{18} values, with a decrease in T_{18} from 120 to 220 °C (Fig. 9). While the mechanism for this shift is unknown, we suspect that liquid hydrocarbons in the sample cylinders may retain some methane, and that this absorption or dissolution causes an isotopic fractionation leading to apparently high temperatures. In contrast, a sample of mixed thermogenic and microbial gas from the Gulf of Mexico, which indicated a significantly lower T_{18} value (70 ± 9 °C) when originally extracted at room temperature, did not show a significantly different T_{18} value (58 ± 8 °C) when extracted at 85 °C (Fig. 9). The gas in this cylinder was at a lower pressure, and therefore C_{4+}hydrocarbons were less likely to be liquids and to adsorb methane. Most samples discussed here were not stored in high-pressure cylinders

containing significant quantities of C_{4+} hydrocarbons, and this is unlikely to be an issue for our interpretation of Δ_{18} data, except in the cases of the Eagleford and Bakken shale samples. Regardless, we recommend that all samples from natural gas reservoirs with substantial C_{4+} components stored at high pressures be heated during extraction to avoid this effect.

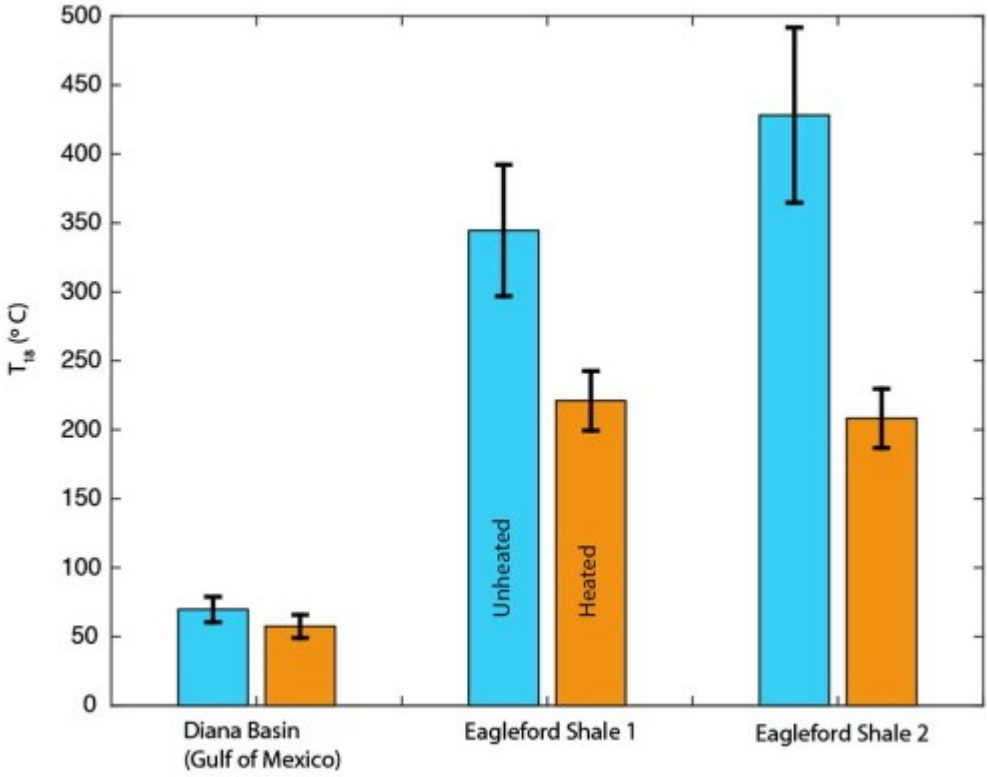

Fig. 9. Plot shows the difference in T_{18} values for three natural gas samples between methane extracted without heating the steel cylinder and methane extracted while heating the cylinder to 85 °C. In a sample from the Gulf of Mexico with a relatively low T_{18} value the difference between treatments is within error. For two samples from the Eagleford Shale, however, heating the sample cylinder led to substantially lower T_{18} values.

Second, high clumped isotope temperatures may be the result of secondary isotope effects related to methane transport, either occurring naturally or as a result of oil and gas extraction. Gas diffusion, in particular, is predicted to decrease Δ_{18} values in the residual gas. For example, diffusive loss of 30% of the methane in a reservoir, assuming inter-gas diffusion in air, would cause the residual methane Δ_{18} to increase by 0.6‰. If methane originally formed at 230 °C (Δ_{18} of 2.3‰), this diffusive loss would lead to an increase in T_{18}values to 305 °C (Δ_{18} of 1.7‰) (Section 3.4). The high apparent temperatures measured for some methane samples could thus indicate that the analyzed sample is residual gas remaining in the source or reservoir rock after diffusive loss of a significant fraction of the total gas in the reservoir. We note, however, that inter-gas diffusion is not a realistic model for petroleum systems, and that isotope effects for diffusion through permeable rock or liquid are poorly constrained (Prinzhofer and Huc, 1995, Zhang and Krooss, 2001), and unknown for clumped isotopes. It is

unknown whether either hydraulic fracturing or subsequent gas separation induce measurable isotopic fractionations, and it is possible that these production processes could also contribute to high T_{18} values.

Third, high temperature cracking experiments have in some cases produced methane with T_{18} values that are significantly higher than the experimental temperature (Shuai et al., in revision), as discussed above in Section 3.2. These data may indicate that thermogenic cracking of sedimentary organic matter can produce methane with non-equilibrium Δ_{18}values under specific circumstances, and that high apparent temperatures in some systems could be a result of this non-equilibrium isotope effect.

Finally, high T_{18} values could represent true formation temperatures for methane originating at greater depths than is currently predicted by models of oil and gas generation (Seewald, 2003). The variability in T_{18} values observed in many of the studied sedimentary basins might then reflect differential contributions of methane from shallow versus deep environments.

The heated cylinder extraction and non-equilibrium results from pyrolysis experiments raise the possibility that analytical artifacts or kinetic isotope effects during methane generation may be responsible for some of the highest apparent temperatures that have been observed. Furthermore, isotope effects during gas diffusion or separation may also possibly alter Δ_{18} signals, although the signature of these processes has not been clearly identified in natural samples. It remains to be seen whether evidence supports methane forming at temperatures greater than 300 °C and whether this represents a substantial contribution to natural gas reservoirs.

4.6. Mixing of methane from distinct sources

Mixtures of methane from different sources are common in natural gas reservoirs and seeps (Schoell, 1983). Clumped isotope data can provide new insights into such mixtures and the characteristics of the end-members, and serve as a basis for quantitative apportionment. As discussed above, mixing can be non-linear in Δ_{18} or $\Delta^{13}CH_3D$ values (Section 2.3, Fig. 4), with the non-linearity becoming increasingly pronounced as the difference in δD and $\delta^{13}C$ values between the end-members becomes larger. An example of clumped isotope analyses to constrain methane mixing is in the Antrim Shale of Michigan (Stolper et al., 2015). Previously, hydrogen isotope ratios were interpreted as indicating that the methane in this shale was dominantly (>80%) microbial, though thermogenic gas is also clearly present in the basin based on significant quantities (~20% in some samples) of C_{2+} hydrocarbons (Martini et al., 1996). The clumped isotope data, however, indicate two end-members of methane, one forming around 140 °C or above, which is above the known range of microbial methanogenesis, while the other formed at temperatures around 20 °C (Stolper et al., 2015) (Fig. 10). Subsequent analysis of noble gas concentrations further support the

contribution of significant quantities of thermogenic methane to the Antrim Shale gas reservoir (Wen et al., 2015).

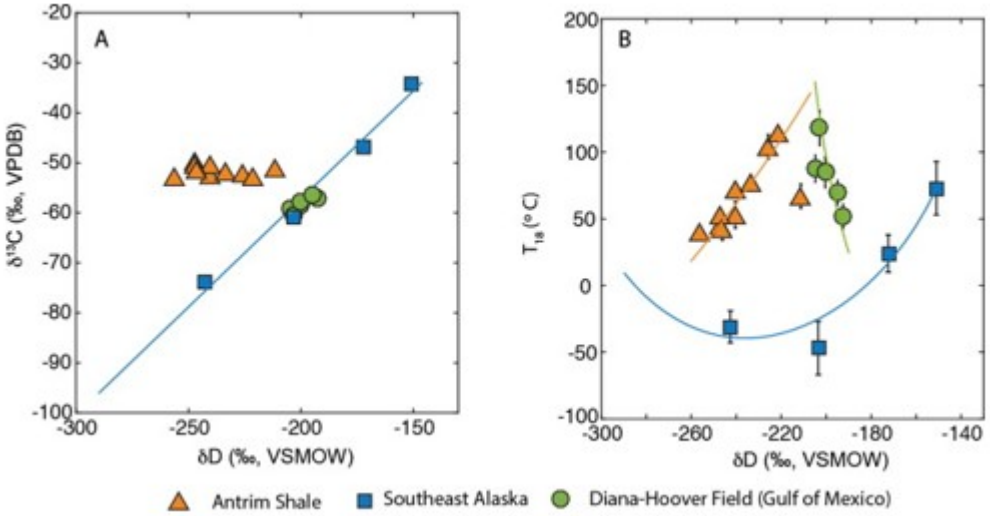

Fig. 10. Plots of (A) δD vs. $\delta^{13}C$ and (B) δD vs. T_{18} for three suites of gases inferred to be mixtures of methane from high- and low-temperature formation environments. Mixing models for the Antrim Shale(Stolper et al., 2015) and Southeast Alaska (Douglas et al., 2016) were described previously. The mixing trend for the Diana/Hoover Fields was based on end-members from inferred pure microbial (Stolper et al., 2014b) and thermogenic methane (this study) from nearby fields in the Gulf of Mexico. The non-linearityof mixing of T_{18} values for the Antrim Shale and Diana/Hoover Fields is subtle, but is much more pronounced in Southeast Alaska, where the end-members differ much more in δD and $\delta^{13}C$.

In southeastern Alaska a selection of methane samples emitted from seeps near Lake Eyak also exhibited signs of mixing of methane from distinct formation environments. This mixing was first identified by linear co-variation of δD, $\delta^{13}C$, and $\Delta^{14}C$ values, and was originally thought to reflect mixing of microbial methane produced in lake sediments, and thermogenic methane from underlying strata (Walter Anthony et al., 2012). Clumped isotope analysis revealed elevated Δ_{18} values, which correspond to negative apparent temperatures (i.e., below 0 °C) in two of these samples. The data also exhibit a non-linear trend in Δ_{18}-δD space (Fig. 10). When constrained by ^{14}C data, the Δ_{18}-δD and Δ_{18}-$\delta^{13}C$ two end-member mixing curves fit to these samples suggest a high temperature component that formed at around 60 °C (Douglas et al., 2016). Methane emitted in nearby Prince William Sound has a similar T_{18} value of 73 ± 10 °C, consistent with this formation temperature. These relatively low temperatures, combined with high $[C_1]/[C_2]$ values, suggest that the high-temperature end-member in this setting may originate from deep subsurface microbes instead of thermogenic gas generation (Douglas et al., 2016). These data comprise the first instance in which non-linear mixing of Δ_{18} values in a natural environment results in noticeably elevated Δ_{18} values (Fig. 10), but such an effect is likely to occur in other settings where methane end members produced in deep and surficial environments mix, especially when the δD values of the end-members are substantially different.

Methane in offshore natural gas reservoirs in the Diana-Hoover Field of the Gulf of Mexico yields T_{18} values from 52 to 118 °C (Fig. 10). 118 °C is a plausible thermogenic formation temperature in this environment and is consistent with maturity estimates from biomarkerratios, but the observed lower temperatures are likely the result of mixing with microbial methane produced by oil biodegradation. Methane from the nearby Hadrian South Field, interpreted as resulting from oil biodegradation, yields T_{18} values between 34 and 48 °C, within analytical uncertainty of measured reservoir temperatures (Stolper et al., 2014b), and lower than the values observed in the Diana-Hoover Field. In the Diana-Hoover Field T_{18}inversely correlates with both δD and $\delta^{13}C$ (Fig. 7, Fig. 10), suggesting that the microbial methane component is relatively enriched in D and ^{13}C relative to the thermogenic component. Previous research has shown that thermophilic methanogens (environments between 50 and 75 °C) produce methane with relatively high δD and $\delta^{13}C$ values (Schoell, 1980, Valentine et al., 2004) compared to mesophilic organisms (environments < 50 °C), which could account for this effect. The variable isotopic compositions in the Diana-Hoover Field likely represent differential mixing of thermogenic and microbial methane having similar $\delta^{13}C$ values. Alternatively, this variability be related to the residence time of thermogenic gas and oil in relatively low-temperature reservoirs. Longer residence times may correspond to a greater proportion of microbial methane produced by oil degradation and consequently lower T_{18} values.

Finally, in two samples from Songliao Basin in Eastern China we have also observed very high Δ_{18} values of 6.9‰ and 10.2‰, corresponding to T_{18} temperatures of 5 and −77 °C (Supplementary Table), with the latter Δ_{18} value the highest observed in any sample thus far. These inferred temperatures are much lower than the measured well temperatures (25 and 32 °C, respectively), but are plausible as a result of non-linear variation in Δ_{18} for mixtures of methane end-members having widely differing δD and $\delta^{13}C$ values (Fig. 4, Fig. 10). Methane in these samples was previously inferred to be dominantly microbial with a minor thermogenic component based on carbon isotope and gas composition data (Zhang et al., 2011), a conclusion that is consistent with the observed high Δ_{18} values. However, without additional samples we are unable to provide further constraints on the end-member compositions and their fractional contribution to these samples.

4.7. Deep subsurface microbial methane

Microbial methanogenesis occurs in a number of deep (>100 m below the land surface or seafloor) subsurface environments, including buried organic-rich sediments, coal beds, and oil reservoirs (Wilhelms et al., 2001, Strąpoć et al., 2011, Valentine, 2011). It has been proposed that methanogens survive temperatures up to 80–90 °C (Wilhelms et al., 2001). However, pure-culture incubations demonstrate that methanogens can grow at higher temperatures up to 122 °C, at least under laboratory conditions (Takai et al., 2008). Clumped isotope data exist for microbial methane samples from

several deep subsurface environments, including biodegraded oil reservoirs, terrigenous and marine coal seams, and organic-rich lacustrine shales, and span a range of T_{18} values from 34–95 °C (Fig. 11a).

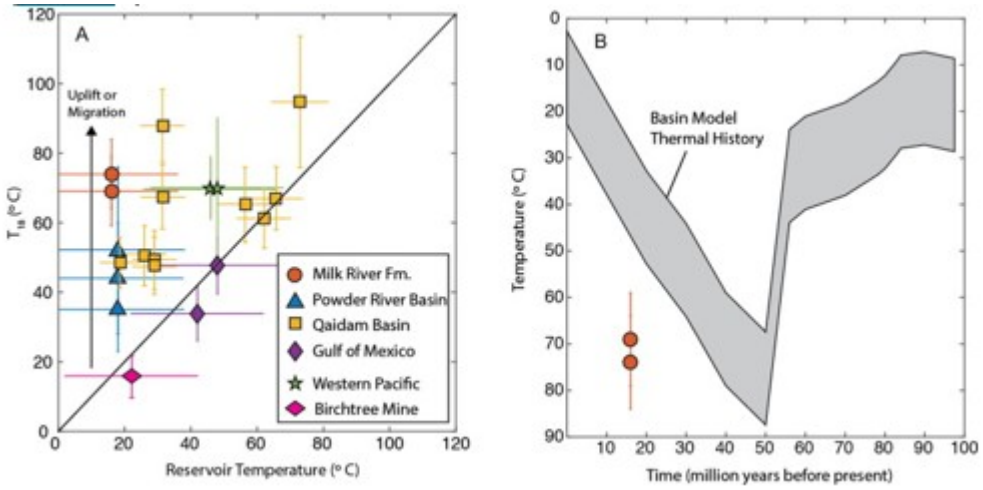

Fig. 11. (A) Comparison of T_{18} values vs. estimated reservoir temperatures for deep subsurface microbial methane samples. T_{18} values are either within error of, or significantly higher than, reservoir temperatures. T_{18} values higher than reservoir temperatures may indicate uplift of methane forming strata to cooler thermal environments, or migration of gas from deeper strata. Methodologies for reservoir temperature measurements or estimates are detailed in Section 2.4. We applied a conservative 20 °C error to reservoir temperatures, with the exception of drill-stem tests from the Qaidam Basin, where we applied a 10% error. (B) Comparison of the thermal history of the Milk River Formation with methane T_{18}values. The T_{18} values suggest that methane predominantly formed during the deepest burial of the sediments, prior to subsequent uplift. Data from Stolper et al., 2014b, Inagaki et al., 2015, Wang et al., 2015, Young et al., 2017; and this study.

T_{18} values from deep subsurface methanogens are generally within error of, or higher than, estimated reservoir temperatures for the sampled gases (Fig. 11a). In cases where T_{18}values exceed the reservoir temperatures it is possible that methane formed at deeper burial depths, and then moved to shallower, cooler environments either through gas migration or uplifting of the strata. For example, methane from the Milk River Formation of Alberta yields T_{18} values for two samples of 69 ± 10 and 74 ± 10 °C, but the current well temperature is estimated to be 12 °C (Fig. 11b). Comparison with a basin thermal model suggests that the T_{18} values are most consistent with methane formation during maximum burial temperatures of the Milk River Formation from 40 to 50 million years ago, between 60 and 87 °C (Fig.11b). A plausible explanation is that methane that formed early in the burial history at cooler temperatures migrated out of the strata prior to lithification, and that only late-formed methane from the deepest burial depths was retained within the strata following lithification. Later, as the formation was uplifted, no new microbial methanogenesis occurred, possibly because lithification made conditions unfavorable for methanogens.

In other settings where methane T_{18} values are higher than reservoir temperatures, such as the Qaidam basin, a similar process can be invoked. It is also possible that there has been migration of gas from deeper methane-

producing strata to overlying strata. Gas migration may be a more likely scenario in the Qaidam Basin, where different wells have widely varying temperatures (from 19 to 73 °C), but in many cases the T_{18} values are higher than the reservoir temperatures. In the uplift or gas migration scenarios there may be significant mixing of methane formed at different temperatures. Additionally, in some cases there may be a component of thermogenic gases in these samples, which could raise the inferred temperatures. Furthermore, we cannot rule out that deviations from reservoir temperatures could be caused by kinetic isotope fractionations during microbial methanogenesis, which have been clearly observed in freshwater and cultured microbial methanogenesis. One sample of putative microbial methane from the Niobrara Formation in Colorado demonstrated slight disequilibrium in $\Delta^{13}CH_3D$-$\Delta^{12}CH_2D_2$ space, which potentially explains a higher than expected T_{13CH3D} value for this sample (142 °C) (Young et al., 2017). Finally, as noted above (Section 2.4) well temperature estimates are approximate, and errors in these values could explain some discrepancies with the T_{18} values, although they are unlikely to account for the largest observed differences (i.e., > 50 °C in the Milk River Formation and Qaidam Basin; Fig. 11).

One further example of deep subsurface microbial methane is a large gas seep (CH_4 flux of 65 L/min) in a permafrost hosted lake on the North Slope of Alaska. The methane emitted from this seep has a T_{18} of 9 ± 10 °C, within error of the temperature of lake sediments (~0 °C). However, the Δ_{18} value is higher than that observed in most other lacustrine methane, as almost all other samples of this type, including from the same region of Alaska, record substantial kinetic fractionations (Wang et al., 2015, Douglas et al., 2016). Additional evidence, including the relatively high δD and $\delta^{13}C$ values for this sample, the absence of ^{14}C, the high methane flux, and the fact that coal seams underlie the lake, all support the hypothesis that the seep emits microbial coal-bed methane formed within or beneath the permafrost, which extends to about 300–400 m below the surface in this area (Walter Anthony et al., 2012).

4.8. Marine microbial methane

Microbial methanogenesis occurs in shallow (<100 m), unlithified marine sediments across the global ocean (Valentine, 2011). Thus far, clumped isotopes have been measured in microbial methane from a number of seeps, pore fluids, and gas hydrates (Stolper et al., 2015, Wang et al., 2015, Douglas et al., 2016). T_{18} values for these samples range from 0 to 42 °C (Fig. 6), almost all of which are within error of seafloor or sediment temperatures. In addition, comparison of $\alpha_{H20\text{-}CH4}$ and Δ_{18} or $\Delta^{13}CH_3D$ values indicates that all marine microbial methane samples analyzed thus far formed at or near isotopic equilibrium, both internally and in terms of hydrogen exchange between water and methane (Fig. 3). The depths at which these methane samples were generated is unknown, but the clumped-isotope temperatures provide bounds on these depths if the local geothermal

gradient is known. In the case of methane sampled from the Beaufort Shelf, where permafrost extends to a depth of 700 m (Paull et al., 2011), methane forming in relatively deep settings could be consistent with inferred formation temperatures that are within error of seafloor temperatures (~0 °C). In this setting the ^{14}C content of methane is much lower than that of sedimentary organic matter, suggesting a deeper, older organic carbon source for methanogenesis.

Gas hydrates sampled from Hydrate Ridge in the North Cascadia Margin record T_{18} values from 12 to 42 °C, whereas sediment temperatures range from 3 to 17 °C (Wang et al., 2015). It is possible that the highest temperature sample represents methane migrated from higher temperature environments, but the δD and $\delta^{13}C$ values of these samples suggest a dominantly microbial source.

A key question in light of these data is why marine microbial methane samples (in addition to deep subsurface microbial methane) seem to form close to equilibrium, whereas freshwater and pure culture microbial methane samples clearly record kinetic fractionations. One possible explanation is that, in the face of competition for substrates by sulfate-reducing microbes, marine methanogenesis is dominantly hydrogenotrophic and strongly substrate (H_2) limited (Valentine, 2011). Such conditions may enhance the reversibility of methanogenesis by reducing the chemical potential gradient between methane and its precursors. This leads more readily to reversibility in the enzymes generating methane by methanogens (Valentine et al., 2004, Conrad, 2005), thus allowing methane to achieve internal isotopic equilibrium via rapid hydrogen exchange with water (Stolper et al., 2015, Wang et al., 2015).

Another possible explanation is that activation of C-H bonds during anaerobic oxidation proceeds reversibly (Hallam et al., 2003) such that C-H bonds are broken and reformed faster than the net rate of methane consumption and methane is re-equilibrated to the temperatures of anaerobic methane oxidation (Stolper et al., 2015). This hypothesis is partially supported by the observation that anaerobic methane oxidation promotes exchange of carbon isotopes between CH_4 and CO_2 (Yoshinaga et al., 2014). If this is the case, Δ_{18}temperatures in marine methane may record the temperature of oxidation rather than formation.

4.9. Freshwater microbial methane

Methane from freshwater environments exhibits a wide range of Δ_{18} values from 9.6 to −1‰ (Fig. 3). The high end of this range corresponds to a T_{18} of −50 °C, while negative Δ_{18}values do not correspond to any temperature. Most methane samples from freshwater environments have low Δ_{18} values that correspond to T_{18} temperatures much hotter than expected based on environmental temperatures (Fig. 6). The exceptions to this pattern include examples discussed above, e.g. methane hypothesized to have been produced in sub-permafrost coal seams, mixtures of thermogenic and

microbial methane emitted from a lake in southeast Alaska, and methane with an elevated Δ_{18} value (9.6‰) from a lake near Fairbanks, Alaska, whose origin is uncertain but could represent the effects of diffusion (Douglas et al., 2016).

These exceptions notwithstanding, the current interpretation of low Δ_{18} values in freshwater microbial methane is that they reflect kinetic isotope fractionations expressed during methane generation related to the differential reversibility of methanogenesis (Stolper et al., 2015, Wang et al., 2015, Douglas et al., 2016), as described in Section 2.2. If this hypothesis is correct, then the variation in Δ_{18} values between samples reflects differences in enzymatic reversibility of methanogens in a given environment. It is possible that some of the observed variability is caused by mixing of methane produced with different kinetic isotope effects, or by post-formation processes, including oxidation and diffusion (Douglas et al., 2016, Wang et al., 2016). Different pathways of methanogenesis may also influence clumped isotope values. For example, it has been hypothesized that the clumped isotope value of methane from fermentative pathways could be partly influenced by isotopic clumping in methyl substrates (Wang et al., 2015, Douglas et al., 2016).

Given that methanogens in freshwater environments can express significant kinetic isotope fractionations during methane generation, clumped isotope measurements in freshwater microbial methane cannot be used to infer formation temperature. However, the wide range of observed Δ_{18} values suggests that such data could provide new insights into the biogeochemistry of freshwater methanogenic environments, and in particular insights into the cell-specific rates of methanogenesis and chemical conditions (e.g., thermodynamicgradients) driving microbial methanogenesis.

In most freshwater microbial methane samples, Δ_{18} and $\Delta^{13}CH_3D$ are negatively correlated with $\alpha_{H20\text{-}CH4}$ (Fig. 3). However, in some cases freshwater samples deviate from the trend predicted by the reversibility model, with lower Δ_{18} values for a given $\alpha_{H20\text{-}CH4}$ value. These deviations may be related to the importance of fermentative methanogenesis pathways in some freshwater environments, since a fermentative methanogen culture experiment expressed a larger deviation in the same direction as that shown by these freshwater samples (Fig. 3) (Douglas et al., 2016). In comparing freshwater biogenic samples from different regions we observe somewhat different trends in Δ_{18} (or $\Delta^{13}CH_3D$) versus $\alpha_{CH4\text{-}H2O}$space. For example, samples from Alaska have lower Δ_{18} for a given $\alpha_{CH4\text{-}H2O}$ relative to samples from lakes and wetlands in Sweden, Massachusetts, and California. It is possible that these trends are an artifact of how water δD values were estimated (Douglas et al., 2016), but it is also possible that they represent differences in either the dominant pathways of methanogenesis or the extent of post-formation oxidation or diffusion in these ecosystems.

5. Potential future applications

5.1. Atmospheric methane

Atmospheric methane is a compelling target for future methane clumped isotope analyses. $\delta^{13}C$ values of atmospheric methane, and to a lesser extent δD and $\Delta^{14}C$ values, have been valuable tools to apportion sources of atmospheric methane (Quay et al., 1999, Fisher et al., 2011, Townsend-Small et al., 2012), and for detecting temporal variability in the strength of those sources (Bousquet et al., 2006, Sapart et al., 2012, Nisbet et al., 2014). However, ambiguities remain in apportioning methane sources based on conventional isotope parameters, and additional isotopic data based on multiply substituted isotopologues could provide further constraints. However, there are analytical challenges facing the development of clumped isotope measurements of atmospheric methane. Currently all of the available measurement techniques require relatively large (between 500 and 50 μmol) and highly purified aliquots of methane (Ono et al., 2014, Stolper et al., 2014a). Analysis of atmospheric methane will require removing N_2 and O_2 from very large atmospheric samples, or measuring methane clumped isotopes in the presence of abundant N_2 and O_2, neither of which has been demonstrated yet.

Despite the lack of atmospheric measurements, there are some theoretical and laboratory constraints on the clumped isotope composition of atmospheric methane (Gierczak et al., 1997, Feilberg et al., 2005, Joelsson et al., 2014, Joelsson et al., 2015, Whitehill et al., 2017). This work suggests that atmospheric chemical reactions cause large enrichments in both $^{12}CH_2D_2$ and $^{13}CH_3D$ relative abundance. The dominant atmospheric methane sink is reaction with $OH\bullet^-$ (~85%, (Kirschke et al., 2013), and laboratory studies indicate a kinetic isotope effect for $^{13}CH_3D$ reacting with $OH\bullet^-$ of 1.343 at tropospheric temperatures (Whitehill et al., 2017), while that for $^{12}CH_2D_2$ reacting with $OH\bullet^-$ is estimated to be 1.81 (Gierczak et al., 1997). Similarly, the observed kinetic effect of $Cl\bullet^-$ reacting with $^{13}CH_3D$ (1.579) (Whitehill et al., 2017) is much smaller than that for $Cl\bullet^-$ reacting with $^{12}CH_2D_2$ (2.45) (Feilberg et al., 2005). The substantially larger kinetic isotope effects for $^{12}CH_2D_2$ suggests that measurements of this isotopologue in atmospheric methane could be useful to constrain the extent of atmospheric sink reactions, and could be used to correct atmospheric methane $\Delta^{13}CH_3D$, δD, and $\delta^{13}C$ values for fractionations related to atmospheric sinks. This correction could be used to more accurately identify the isotopic signatures of atmospheric methane sources. In any analysis of atmospheric methane, non-linear mixing of clumped isotope values will be an important consideration, since the products of complex mixtures involving many methane sources will need to be modeled and constrained. However, it is possible that these non-linear mixing relationships could provide distinctive fingerprints for different categories of mixtures, and help to resolve ambiguities in δD and $\delta^{13}C$ values that can occur in atmospheric mixtures.

Clumped isotopes in methane from ice cores present a second exciting possibility to distinguish past changes in methane sources and sinks. The development of methane ^{14}C measurements in ice samples from the Greenland and Antarctic ice sheets (Petrenko et al., 2008, Petrenko et al., 2009, Petrenko et al., 2016) is promising in this regard, since clumped isotope analyses require similar amounts of sample to ^{14}C measurements. However, as discussed above in regards to atmospheric methane, this application will also require new techniques to purify methane mixed with large concentrations of N_2 and O_2.

5.2. Methane on other planets

Methane is also highly relevant to the study of planetary chemistry beyond Earth. Methane can be a significant component of planetary atmospheres (Atreya et al., 2003, Formisano et al., 2004, Swain et al., 2008, Mumma et al., 2009). For example, methane exists in liquid form on Titan (Lunine and Atreya, 2008). $^{13}CH_3D$ has been detected spectroscopically in Titan's atmosphere, although no $\Delta^{13}CH_3D$ value was calculated (Bézard et al., 2007).

Methane is an attractive target in the search for life on other planets because it can both be produced and consumed by microbes. The detection of methane on Mars, and variations in its atmospheric concentration, has generated great interest as a potential biosignature (Formisano et al., 2004, Oze and Sharma., 2005, Mumma et al., 2009, Webster et al., 2013, Webster et al., 2015). Clumped isotope measurements of Martian methane could be useful to evaluate its origin, since this method can be helpful in differentiating thermogenic, volcanic, abiotic and microbial methane (Fig. 5, Fig. 6). In addition, clumped isotope values do not depend on the δD or $\delta^{13}C$ values, which may be difficult to interpret on another planetary body. With current measurement technology, however, it is difficult to imagine either making a measurement using a deployed instrument on Mars, or returning a sufficiently large sample for a laboratory measurement. For example, measuring Δ_{18} to a precision of ~1‰ in relatively high concentration pulses of methane detected at Gale Crater (7.2 ppb; (Webster et al., 2015) would require approximately 3.5 million liters of Martian atmosphere. However as technologies continue to develop, particularly in terms of spectroscopic measurements, it is possible that this situation could change within the next 10–20 years.

6. Conclusions and outlook

A substantial body of clumped isotope data for methane now exists, and provides a basis for understanding the major biogeochemical controls on this property in nature (Fig. 5). Two distinct processes are recognized, broadly characterized as equilibrium versus kinetic fractionations. Methane appears to form in isotopic equilibrium in a variety of environments, including hydrothermal, thermogenic, abiogenic, and marine microbial methane sources. In these samples, the clumped isotope composition generally

provides insights into sample formation temperature. As discussed above (Section 4.5.1), however, there are several examples of clumped isotope data that yield formation temperatures higher than expected given other independent constraints, and clumped isotope data should always be interpreted in the context of the geological and geothermal conditions of the studied system. In addition, further efforts are needed to constrain the Δ_{18}-T relationship below ~150 °C.

In contrast, many of the microbial methane samples studied so far appear to be affected by kinetic fractionations thought to arise during biosynthesis. Such effects are typically associated with low methane δD values (Fig. 5), and preclude interpreting clumped isotope compositions as formation temperature. However, the data may offer insights into the bioenergetics and reversibility of methanogenesis. Preliminary evidence also indicates the possibility of substantial kinetic effects in the formation of thermogenic and abiotic methane (Young et al., 2017). There is also evidence for clumped isotope fractionations as a result of mixing, aerobic oxidation, and atmospheric sink reactions, but there is little or no data on fractionations due to diffusive transport or anaerobic oxidation.

As analytical techniques for clumped isotope measurement continue to progress, we envision four general fields of application for such data. First, methane clumped isotopes have growing value as a geothermometer to help determine formation conditions and transport pathways for natural gas and associated petroleum (Stolper et al., 2014b, Stolper et al., 2015, Stolper et al., in press). Second, they have potential as a forensic tool to characterize and distinguish point-source emissions of methane. The large and diagnostic differences in Δ_{18} values observed between different natural emissions in Arctic environments (Douglas et al., 2016) provides an example of this type of application. Third, clumped isotope analyses should prove useful to understand the biogeochemistry of methanogenesis and methanotrophy, with a focus on the apparent relationship between kinetic fractionations and the reversibility of biochemical pathways (Stolper et al., 2015, Wang et al., 2015, Douglas et al., 2016, Wang et al., 2016). Fourth, clumped isotope data could prove to be a valuable tracer to identify sources and sinks of atmospheric methane (Joelsson et al., 2015, Whitehill et al., 2017), but as discussed above, there are substantial methodological hurdles that must be cleared before this can be realized.

Acknowledgments

The development of the Ultra was funded by NSF-EAR. PMJD was supported in part by Royal Dutch Shell. Research on the Santa Barbara Basin was supported by NSFOCE-1046144. The manuscript benefitted from constructive reviews from Andrew Murray, Kenneth Peters, and Xinyu Xia.

References

Alexander et al., 1982

R. Alexander, R.I. Kagi, A.V. Larcher**Clay catalysis of aromatic hydrogen-exchange reactions**

Geochimica et Cosmochimica Acta, 46 (1982), pp. 219-222

Alexander et al., 1984

R. Alexander, R.I. Kagi, A.V. Larcher**Clay catalysis of alkyl hydrogen exchange reactions—reaction mechanisms**

Organic Geochemistry, 6 (1984), pp. 755-760

Alperin et al., 1988

M. Alperin, W. Reeburgh, M. Whiticar**Carbon and hydrogen isotope fractionation resulting from anaerobic methane oxidation**

Global Biogeochemical Cycles, 2 (1988), pp. 279-288

Atreya et al., 2003

S. Atreya, P. Mahaffy, H. Niemann, M. Wong, T. Owen**Composition and origin of the atmosphere of Jupiter—an update, and implications for the extrasolar giant planets**

Planetary and Space Science, 51 (2003), pp. 105-112

Atreya et al., 2007

S.K. Atreya, P.R. Mahaffy, A.-S. Wong**Methane and related trace species on Mars: origin, loss, implications for life, and habitability**

Planetary and Space Science, 55 (2007), pp. 358-369

Bates et al., 2011

B.L. Bates, J.C. McIntosh, K.A. Lohse, P.D. Brooks**Influence of groundwater flowpaths, residence times and nutrients on the extent of microbial methanogenesis in coal beds: powder River Basin, USA**

Chemical Geology, 284 (2011), pp. 45-61

Bernard et al., 1978

B.B. Bernard, J.M. Brooks, W.M. Sackett**Light hydrocarbons in recent Texas continental shelf and slope sediments**

Journal of Geophysical Research: Oceans, 83 (1978), pp. 4053-4061

Bézard et al., 2007

B. Bézard, C.A. Nixon, I. Kleiner, D.E. Jennings**Detection of $^{13}CH_3D$ on Titan**

Icarus, 191 (2007), pp. 397-400

Borrel et al., 2011

G. Borrel, D. Jézéquel, C. Biderre-Petit, N. Morel-Desrosiers, J.-P. Morel, P. Pey ret, G. Fonty, A.-C. Lehours**Production and consumption of methane in freshwater lake ecosystems**

Research in Microbiology, 162 (2011), pp. 832-847

Bousquet et al., 2006

P. Bousquet, P. Ciais, J. Miller, E. Dlugokencky, D. Hauglustaine, C. Prigent, G. Van der Werf, P. Peylin, E.-G. Brunke, C. Carouge**Contribution of anthropogenic and natural sources to atmospheric methane variability**

Nature, 443 (2006), pp. 439-443

Bui et al., 2014

T.Q. Bui, L. Shen, D. Hogan, P. Chen, M. Okumura**Dual Wavelength Cavity Ringdown Spectroscopy for High Precision Methane Isotope Ratio Measurements, 69th International Symposium on Molecular Spectroscopy**

University of Illinois at Champaign-Urbana, Champaign-Urbana, IL (2014)

Chanton, 2005

J.P. Chanton**The effect of gas transport on the isotope signature of methane in wetlands**

Organic Geochemistry, 36 (2005), pp. 753-768

Clog et al., 2015

M. Clog, R. Ellam, A. Hilkert, J. Schwieters, D. Hamilton**New Developments in High-resolution Gas Source Isotope Ratio Mass Spectrometers, American Geophysical Union 2015 Fall Meeting**

American Geophysical Union, San Francisco (2015)

Coleman et al., 1995

D.D. Coleman, C.-L. Liu, K.C. Hackley, S.R. Pelphrey**Isotopic identification of landfill methane**

Environmental Geosciences, 2 (1995), pp. 95-103

Conrad, 2005

R. Conrad**Quantification of methanogenic pathways using stable carbon isotopic signatures: a review and a proposal**

Organic Geochemistry, 36 (2005), pp. 739-752

Coplen, 2011

T.B. Coplen**Guidelines and recommended terms for expression of stable-isotope-ratio and gas-ratio measurement results**

Rapid Communications in Mass Spectrometry, 25 (2011), pp. 2538-2560

Curtis, 2002

J.B. Curtis**Fractured shale-gas systems**

American Association of Petroleum Geologists Bulletin, 86 (2002), pp. 1921-1938

Daëron et al., 2011

M. Daëron, W. Guo, J. Eiler, D. Genty, D. Blamart, R. Boch, R. Drysdale, R. Mai re, K.Wainer, G. Zanchetta**$^{13}C^{18}O$ clumping in speleothems: observations from natural caves and precipitation experiments**

Geochimica et Cosmochimica Acta, 75 (2011), pp. 3303-3317

Daniels et al., 1980

L. Daniels, G. Fulton, R. Spencer, W. Orme-Johnson**Origin of hydrogen in methane produced by *Methanobacterium thermoautotrophicum***

Journal of Bacteriology, 141 (1980), pp. 694-698

Denman et al., 2007

Denman, K.L., Brasseur, G.P., Chidthaisong, A., Ciais, P., Cox, P.M., Dickinson, R.E., Hauglustaine, D.A., Heinze, C., Holland, E.A., Jacob, D.J., Lohmann, U., Ramachandran, S., da Silva Dias, S.C., Wofsy, S.C., Zhang X., 2007. Couplings between changes in the climate system and biogeochemistry. In: Solomon, S., Qin, D., Manning, M., Chen, Z., Marquis, M., Averyt, K.B., Tignor, M., Miller, H.L. (Eds.). Climate Change 2007: The Physical Science Basis. Contribution of Working Group I to the Fourth Assessment Report of the Intergovernmental Panel on Climate Change. Cambridge University Press, Cambridge, UK, and New York, NY, USA.

Douglas et al., 2016

P. Douglas, D. Stolper, D. Smith, Anthony
K. Walter, C. Paull, S. Dallimore, M. Wik, P. Crill, M. Winterdahl, J. Eiler, A.L. Se ssions**Diverse origins of Arctic and Subarctic methane point source emissions identified with multiply-substituted isotopologues**

Geochimica et Cosmochimica Acta, 188 (2016), pp. 163-188

Eiler, 2013

J. Eiler**The isotopic anatomies of molecules and minerals**

Annual Review of Earth and Planetary Sciences, 41 (2013), pp. 411-441

Eiler, 2007

J.M. Eiler**“Clumped-isotope” geochemistry – the study of naturally-occurring, multiply-substituted isotopologues**

Earth and Planetary Science Letters, 262 (2007), pp. 309-327

Eiler et al., 2014

Eiler, J.M., Blake, G., Dallas, B., Kitchen, N., Lloyd, M., Sessions, A.L., 2014. Isotopic Anatomies of Organic Compounds, Goldschmidt Conference, Sacramento CA.

Eiler et al., 2013

J.M. Eiler, M. Clog, P. Magyar, A. Piasecki, A. Sessions, D. Stolper, M. Deerberg, H.-J.Schlueter, J. Schwieters**A high-resolution gas-source isotope ratio mass spectrometer**

International Journal of Mass Spectrometry, 335 (2013), pp. 45-56

Eiler and Schauble, 2004

J.M. Eiler, E.A. Schauble**$^{18}O^{13}C^{16}O$ in Earth's atmosphere**

Geochimica Et Cosmochimica Acta, 68 (2004), pp. 4767-4777

Emmanuel and Ague, 2007

S. Emmanuel, J.J. Ague**Implications of present-day abiogenic methane fluxes for the early Archean atmosphere**

Geophysical Research Letters, 34 (2007), p. L15810

Etiope et al., 2009

G. Etiope, A. Feyzullayev, A.V. Milkov, A. Waseda, K. Mizobe, C.H. Sun**Evidence of subsurface anaerobic biodegradation of hydrocarbons and potential secondary methanogenesis in terrestrial mud volcanoes**

Marine and Petroleum Geology, 26 (2009), pp. 1692-1703

Etiope, 2012

G. Etiope**Methane uncovered**

Nature Geoscience, 5 (2012), pp. 373-374

Etiope, 2015

G. Etiope**Natural Gas Seepage: The Earth’s Hydrocarbon Degassing**

Springer, Cham, Switzerland (2015)

Etiope et al., 2008

Etiope, G., Lassey, K.R., Klusman, R.W., Boschi, E., 2008. Reappraisal of the fossil methane budget and related emission from geologic sources. Geophysical Research Letters 35.

Etiope and Schoell, 2014

G. Etiope, M. Schoell**Abiotic gas: atypical, but not rare**

Elements, 10 (2014), pp. 291-296

Etiope et al., 2011

G. Etiope, M. Schoell, H. Hosgörmez**Abiotic methane flux from the Chimaera seep and Tekirova ophiolites (Turkey): understanding gas exhalation from low temperature serpentinization and implications for Mars**

Earth and Planetary Science Letters, 310 (2011), pp. 96-104

Etiope and Sherwood Lollar, 2013

G. Etiope, B. Sherwood Lollar**Abiotic methane on Earth**

Reviews of Geophysics, 51 (2013), pp. 276-299

Etiope et al., 2013

G. Etiope, B. Tsikouras, S. Kordella, E. Ifandi, D. Christodoulou, G. Papatheod orou**Methane flux and origin in the Othrys ophiolite hyperalkaline springs, Greece**

Chemical Geology, 347 (2013), pp. 161-174

Etiope et al., 2016

G. Etiope, I. Vadillo, M. Whiticar, J. Marques, P. Carreira, I. Tiago, J. Benavente , P. Jiménez, B. Urresti**Abiotic methane seepage in the Ronda peridotite massif, southern Spain**

Applied Geochemistry, 66 (2016), pp. 101-113

Feilberg et al., 2005

K.L. Feilberg, D.W. Griffith, M.S. Johnson, C.J. Nielsen**The ^{13}C and D kinetic isotope effects in the reaction of CH_4 with Cl**

International Journal of Chemical Kinetics, 37 (2005), pp. 110-118

Ferry, 1993

Ferry, J.G., 1993. Fermentation of acetate. In: Methanogenesis (Ed.J.G. Ferry). Springer, New York, NY. pp. 304–334.

Fiebig et al., 2004

J. Fiebig, G. Chiodini, S. Caliro, A. Rizzo, J. Spangenberg, J.C. Hunziker**Chemic al and isotopic equilibrium between CO_2 and CH_4 in fumarolic gas discharges: generation of CH_4 in arc magmatic-hydrothermal systems**

Geochimica et Cosmochimica Acta, 68 (2004), pp. 2321-2334

Fiebig et al., 2015

J. Fiebig, S. Hofmann, F. Tassi, W. D'Alessandro, O. Vaselli, A.B. Woodland**Iso topic patterns of hydrothermal hydrocarbons emitted from Mediterranean volcanoes**

Chemical Geology, 396 (2015), pp. 152-163

Fiebig et al., 2013

J. Fiebig, F. Tassi, W. D'Alessandro, O. Vaselli, A.B. Woodland**Carbon-bearing gas geothermometers for volcanic-hydrothermal systems**

Chemical Geology, 351 (2013), pp. 66-75

Fisher et al., 2011

R.E. Fisher, S. Sriskantharajah, D. Lowry, M. Lanoisellé, C. Fowler, R. James, O. Hermansen, Myhre C. Lund, A. Stohl, J. Greinert, E.G. Nisbet**Arctic methane sources: isotopic evidence for atmospheric inputs**

Geophysical Research Letters, 38 (2011), p. L21803

Formisano et al., 2004

V. Formisano, S. Atreya, T. Encrenaz, N. Ignatiev, M. Giuranna**Detection of methane in the atmosphere of Mars**

Science, 306 (2004), pp. 1758-1761

Ghosh et al., 2006

P. Ghosh, J. Adkins, H. Affek, B. Balta, W.F. Guo, E.A. Schauble, D. Schrag, J.M. Eller**13C–18O bonds in carbonate minerals: a new kind of paleothermometer**

Geochimica Et Cosmochimica Acta, 70 (2006), pp. 1439-1456

Gierczak et al., 1997

T. Gierczak, R.K. Talukdar, S.C. Herndon, G.L. Vaghjiani, A. Ravishankara**Rate coefficients for the reactions of hydroxyl radicals with methane and deuterated methanes**

Journal of Physical Chemistry A, 101 (1997), pp. 3125-3134

Gupta et al., 2013

V. Gupta, K.A. Smemo, J.B. Yavitt, D. Fowle, B. Branfireun, N. Basiliko**Stable isotopes reveal widespread anaerobic methane oxidation across latitude and peatland type**

Environmental Science and Technology, 47 (2013), pp. 8273-8279

Hallam et al., 2003

S.J. Hallam, P.R. Girguis, C.M. Preston, P.M. Richardson, E.F. DeLong**Identification of methyl coenzyme M reductase A (*mcrA*) genes associated with methane-oxidizing archaea**

Applied and Environment Microbiology, 69 (2003), pp. 5483-5491

Hermanrud et al., 1991

C. Hermanrud, I. Lerche, K.K. Meisingset**Determination of virgin rock temperature from drillstem tests**

Journal of Petroleum Technology, 43 (1991), pp. 1126-1131

Holler et al., 2011

T. Holler, G. Wegener, H. Niemann, C. Deusner, T.G. Ferdelman, A. Boetius, B. Brunner, F.Widdel**Carbon and sulfur back flux during anaerobic microbial oxidation of methane and coupled sulfate reduction**

Proceedings of the National Academy of Sciences, 108 (2011), pp. E1484-E1490

Horita, 2001

J. Horita**Carbon isotope exchange in the system CO_2-CH_4 at elevated temperatures**

Geochimica et Cosmochimica Acta, 65 (2001), pp. 1907-1919

Horita and Berndt, 1999

J. Horita, M.E. Berndt**Abiogenic methane formation and isotopic fractionation under hydrothermal conditions**

Science, 285 (1999), pp. 1055-1057

Hornafius et al., 1999

J.S. Hornafius, D. Quigley, B.P. Luyendyk**The world's most spectacular marine hydrocarbon seeps (Coal Oil Point, Santa Barbara Channel, California): quantification of emissions**

Journal of Geophysical Research: Oceans, 104 (1999), pp. 20703-20711

Hornibrook et al., 1997

E.R. Hornibrook, F.J. Longstaffe, W.S. Fyfe**Spatial distribution of microbial methane production pathways in temperate zone wetland soils: stable carbon and hydrogen isotope evidence**

Geochimica et Cosmochimica Acta, 61 (1997), pp. 745-753

Hunt, 1979

M. Hunt**Petroleum Geochemistry and Geology**

WH Freeman New York, NY (1979)

IEA, 2015

IEA, 2015. Key World Energy Statistics. Organisation for Economic Co-operation and Development.

Inagaki et al., 2015

F. Inagaki, K.-U. Hinrichs, Y. Kubo, M. Bowles, V. Heuer, W.-L. Hong, T. Hoshino, A. Ijiri, H.Imachi, M. Ito, M. Kaneko, M.A. Lever, Y.-S. Lin, B.A. Methé, S. Morita, Y. Morona, W. Tanikawa, M.Bihan, S.A. Bowden, M. Elvert, C. Glombitza, D. Gross, G.J. Harrington, T. Hori, K. Li, D. Limmer, C.-H.Liu, N. Murayama, S. Ohkouchi, S. Ono, Y.-S. Park, S.C. Phillips, X. Prieto-Mollar, M. Purkey, N.Riedinger, Y. Sanada, J. Sauvage, G. Snyder, R. Susilawati, Y. Takano, E. Tasumi, T. Terada, H. Tomaru, E. Trembath-Reichert, D.T. Wang, Y. Yamada**Exploring**

deep microbial life in coal-bearing sediment down to~ 2.5 km below the ocean floor

Science, 349 (2015), pp. 420-424

James, 1983

A.T. James**Correlation of natural gas by use of carbon isotopic distribution between hydrocarbon components**

American Association of Petroleum Geologists Bulletin, 67 (1983), pp. 1176-1191

Joelsson et al., 2015

L. Joelsson, J.A. Schmidt, E. Nilsson, T. Blunier, D. Griffith, S. Ono, M.S. Johnso n**Development of a new methane tracer: kinetic isotope effect of $^{13}CH_3D$ + OH from 278 to 313 K**

Atmospheric Chemistry and Physics Discussions, 15 (2015), pp. 27853-27875

Joelsson et al., 2014

L.M.T. Joelsson, R. Forecast, J.A. Schmidt, C. Meusinger, E. Nilsson, S. Ono, M. S.Johnson**Relative rate study of the kinetic isotope effect in the $^{13}CH_3D$ + Cl reaction**

Chemical Physics Letters, 605 (2014), pp. 152-157

Khalil and Rasmussen, 1983

M. Khalil, R. Rasmussen**Sources, sinks, and seasonal cycles of atmospheric methane**

Journal of Geophysical Research: Oceans, 88 (1983), pp. 5131-5144

Kirschke et al., 2013

S. Kirschke, P. Bousquet, P. Ciais, M. Saunois, J.G. Canadell, E.J. Dlugokencky, P.Bergamaschi, D. Bergmann, D.R. Blake, L. Bruhwiler**Three decades of global methane sources and sinks**

Nature Geoscience, 6 (2013), pp. 813-823

Krasnopolsky et al., 2004

V.A. Krasnopolsky, J.P. Maillard, T.C. Owen**Detection of methane in the martian atmosphere: evidence for life?**

Icarus, 172 (2004), pp. 537-547

Krooss et al., 1992

B. Krooss, D. Leythaeuser, R. Schafer**The quantification of diffusive hydrocarbon losses through cap rocks of natural gas reservoirs—a re-evaluation: reply**

American Association of Petroleum Geologists Bulletin, 76 (1992), pp. 1842-1846

Lacroix, 1993

A.V. Lacroix**Unaccounted-for sources of fossil and isotopically-enriched methane and their contribution to the emissions inventory: a review and synthesis**

Chemosphere, 26 (1993), pp. 507-557

Le Mer and Roger, 2001

J. Le Mer, P. Roger**Production, oxidation, emission and consumption of methane by soils: a review**

European Journal of Soil Biology, 37 (2001), pp. 25-50

Lowe et al., 1988

D.C. Lowe, C.A. Brenninkmeijer, M.R. Manning, R. Sparks, G. Wallace**Radiocarbon determination of atmospheric methane at Baring Head, New Zealand**

Nature, 332 (1988), pp. 522-525

Lunine and Atreya, 2008

J.I. Lunine, S.K. Atreya**The methane cycle on Titan**

Nature Geoscience, 1 (2008), pp. 159-164

Magyar et al., 2016

P.M. Magyar, V.J. Orphan, J.M. Eiler**Measurement of rare isotopologues of nitrous oxide by high-resolution multi-collector mass spectrometry**

Rapid Communications in Mass Spectrometry, 30 (2016), pp. 1923-1940

Martell, 1963

E. Martell**On the inventory of artificial tritium and its occurrence in atmospheric methane**

Journal of Geophysical Research, 68 (1963), pp. 3759-3770

Martini et al., 1998

A. Martini, L. Walter, J. Budai, T. Ku, C. Kaiser, M. Schoell**Genetic and temporal relations between formation waters and biogenic methane: Upper Devonian Antrim Shale, Michigan Basin, USA**

Geochimica et Cosmochimica Acta, 62 (1998), pp. 1699-1720

Martini et al., 1996

A.M. Martini, J.M. Budai, L.M. Walter, M. Schoell**Microbial generation of economic accumulations of methane within a shallow organic-rich shale**

Nature, 383 (1996), pp. 155-158

McCollom, 2013

T.M. McCollom**Laboratory simulations of abiotic hydrocarbon formation in Earth's deep subsurface**

Reviews in Mineralogy and Geochemistry, 75 (2013), pp. 467-494

McCollom and Seewald, 2013

T.M. McCollom, J.S. Seewald**Serpentinites, hydrogen, and life**

Elements, 9 (2013), pp. 129-134

Moran et al., 2017

Moran, J.J., Whitmore, L.M., Jay, Z.J., Jennings, R.d.M., Beam, J.P., Kreuzer, H.W., Inskeep, W.P., 2017. Dual stable isotopes of CH_4 from Yellowstone hot-springs suggest hydrothermal processes involving magmatic CO_2. Journal of Volcanology and Geothermal Research.

Morrill et al., 2013

P.L. Morrill, J.G. Kuenen, O.J. Johnson, S. Suzuki, A. Rietze, A.L. Sessions, M.L. Fogel, K.H.Nealson**Geochemistry and geobiology of a present-day serpentinization site in California: the cedars**

Geochimica et Cosmochimica Acta, 109 (2013), pp. 222-240

Mumma et al., 2009

M.J. Mumma, G.L. Villanueva, R.E. Novak, T. Hewagama, B.P. Bonev, M.A. DiS anti, A.M.Mandell, M.D. Smith**Strong release of methane on Mars in northern summer 2003**

Science, 323 (2009), pp. 1041-1045

Myhre et al., 2013

Myhre, G.D., Shindell, D.F.-M.B., Collins, W., Fuglestvedt, J., Huang, J., Koch, D., Lamarque, J.-F.D.L., Mendoza, B., Nakajima, T., Robock, A., Stephens, G., Takemura, T., Zhang, H., 2013. Anthropogenic and natural radiative forcing. In: Stocker, T.F., Qin, G.-K., Plattner, G.-K., Tignor, M., Allen, S.K., Boschung, J., Nauels, A., Xia, Y., Bex, V., Midgley, P.M. (Eds.). Climate Change 2013: The Physical Science Basis. Contribution of Working Group I to the Fifth Assessment Report of the Intergovernmental Panel on Climate Change. Cambridge University Press, Cambridge, U.K. pp. 659–740.

Ni et al., 2011

Y. Ni, Q. Ma, G.S. Ellis, J. Dai, B. Katz, S. Zhang, Y. Tang**Fundamental studies on kinetic isotope effect (KIE) of hydrogen isotope fractionation in natural gas systems**

Geochimica et Cosmochimica Acta, 75 (2011), pp. 2696-2707

Nisbet et al., 2014

E.G. Nisbet, E.J. Dlugokencky, P. Bousquet**Methane on the rise—again**

Science, 343 (2014), pp. 493-495

Nunn, 2012

J.A. Nunn**Burial and thermal history of the Haynesville shale: Implications for overpressure, gas generation, and natural hydrofracture**

Gulf Coast Association of Geological Societies Journal, 1 (2012), pp. 81-96

Ono et al., 2014

S. Ono, D.T. Wang, D.S. Gruen, Lollar
B. Sherwood, M. Zahniser, B.J. McManus, D.D. Nelson**Measurement of a doubly-substituted methane isotopologue, $^{13}CH_3D$, by Tunable Infrared Laser Direct Absorption Spectroscopy**

Analytical Chemistry, 86 (2014), pp. 6487-6494

Oze and Sharma., 2005

Oze, C., Sharma, M., 2005. Have olivine, will gas: serpentinization and the abiogenic production of methane on Mars. Geophysical Research Letters 32.

Paull et al., 2011

Paull, C., Dallimore, S., Hughes-Clarke, J., Blasco, S., Lundsten, E., Ussler, W., Graves, D., Sherman, A., Conway, K., Melling, H., Vagle, S., Collett, T., 2011. Tracking the decomposition of submarine permafrost and gas hydrate under the shelf and slope of the Beaufort Sea. In: 7th International Conference on Gas Hydrates. Royal Dutch Shell, Edinburgh, UK.

Penning et al., 2005

H. Penning, C.M. Plugge, P.E. Galand, R. Conrad**Variation of carbon isotope fractionation in hydrogenotrophic methanogenic microbial cultures and environmental samples at different energy status**

Global Change Biology, 11 (2005), pp. 2103-2113

Peters and Nelson, 2012

K. Peters, P.H. Nelson**Criteria to determine borehole formation temperatures for calibration of basin and petroleum system models**

Society for Sedimentary Geology Special Publication, 103 (2012), pp. 5-15

Peters et al., 2015

Peters, K., Xia, X., Pomerantz, A., Mullins, O., 2015. Geochemistry applied to evaluation of unconventional resources. In: Ma, Z., Holditch, S. (Eds.). Unconventional Oil and Gas Resources Handbook: Evaluation and Development. Elsevier, Amsterdam. pp. 71–126.

Petrenko et al., 2008

V.V. Petrenko, J.P. Severinghaus, E.J. Brook, J. Mühle, M. Headly, C.M. Harth, H.Schaefer, N. Reeh, R.F. Weiss, D. Lowe**Instruments and methods: a novel method for obtaining very large ancient air samples from ablating glacial ice for analyses of methane radiocarbon**

Journal of Glaciology, 54 (2008), pp. 233-244

Petrenko et al., 2016

V.V. Petrenko, J.P. Severinghaus, H. Schaefer, A.M. Smith, T. Kuhl, D. Baggen stos, Q.Hua, E.J. Brook, P. Rose, R. Kulin, T. Bauska**Measurements of ^{14}C in ancient ice from Taylor Glacier, Antarctica constrain in situ cosmogenic $^{14}CH_4$ and ^{14}CO production rates**

Geochimica et Cosmochimica Acta, 177 (2016), pp. 62-77

Petrenko et al., 2009

V.V. Petrenko, A.M. Smith, E.J. Brook, D. Lowe, K. Riedel, G. Brailsford, Q. Hua , H.Schaefer, N. Reeh, R.F. Weiss**$^{14}CH_4$ measurements in Greenland ice: investigating last glacial termination CH_4 sources**

Science, 324 (2009), pp. 506-508

Pine and Barker, 1956

M.J. Pine, H. Barker**Studies on the methane fermentation XII: the pathway of hydrogen in the acetate fermentation**

Journal of Bacteriology, 71 (1956), pp. 644-648

Prinzhofer and Pernaton, 1997

A. Prinzhofer, E. Pernaton**Isotopically light methane in natural gas: bacterial imprint or diffusive fractionation?**

Chemical Geology, 142 (1997), pp. 193-200

Prinzhofer and Huc, 1995

A.A. Prinzhofer, A.Y. Huc**Genetic and post-genetic molecular and isotopic fractionations in natural gases**

Chemical Geology, 126 (1995), pp. 281-290

Proskurowski et al., 2008

G. Proskurowski, M.D. Lilley, J.S. Seewald, G.L. Früh-Green, E.J. Olson, J.E. Lup ton, S.P. Sylva, D.S. Kelley**Abiogenic hydrocarbon production at Lost City hydrothermal field**

Science, 319 (2008), pp. 604-607

Quay et al., 1999

P. Quay, J. Stutsman, D. Wilbur, A. Snover, E. Dlugokencky, T. Brown**The isotopic composition of atmospheric methane**

Global Biogeochemical Cycles, 13 (1999), pp. 445-461

Quigley and Mackenzie, 1988

T. Quigley, A. Mackenzie**The temperatures of oil and gas formation in the sub-surface**

Nature, 333 (1988), pp. 549-552

Reeves et al., 2014

E.P. Reeves, J.M. McDermott, J.S. Seewald**The origin of methanethiol in midocean ridge hydrothermal fluids**

Proceedings of the National Academy of Sciences, 111 (2014), pp. 5474-5479

Russell et al., 2010

M. Russell, A. Hall, W. Martin**Serpentinization as a source of energy at the origin of life**

Geobiology, 8 (2010), pp. 355-371

Sackett, 1978

W.M. Sackett**Carbon and hydrogen isotope effects during the thermocatalytic production of hydrocarbons in laboratory simulation experiments**

Geochimica et Cosmochimica Acta, 42 (1978), pp. 571-580

Saenger et al., 2012

C. Saenger, H.P. Affek, T. Felis, N. Thiagarajan, J.M. Lough, M. Holcomb**Carbo nate clumped isotope variability in shallow water corals: temperature dependence and growth-related vital effects**

Geochimica et Cosmochimica Acta, 99 (2012), pp. 224-242

Sapart et al., 2012

C.J. Sapart, G. Monteil, M. Prokopiou, R.S.W. van de Wal, J.O. Kaplan, P. Sperlich, K.M.Krumhardt, C. van der Veen, S. Houweling, M.C. Krol, T. Blunier, T. Sowers, P. Martinerie, E. Witrant, D.Dahl-Jensen, T. Rockmann**Natural and anthropogenic variations in methane sources during the past two millennia**

Nature, 490 (2012), pp. 85-88

Saueressig et al., 2001

G. Saueressig, J.N. Crowley, P. Bergamaschi, C. Brühl, C.A. Brenninkmeijer, H. Fischer**Carbon 13 and D kinetic isotope effects in the reactions of CH_4 with O (^{1} D) and OH: new laboratory measurements and their implications for the isotopic composition of stratospheric methane**

Journal of Geophysical Research: Atmospheres, 106 (2001), pp. 23127-23138

Schoell, 1980

M. Schoell**The hydrogen and carbon isotopic composition of methane from natural gases of various origins**

Geochimica et Cosmochimica Acta, 44 (1980), pp. 649-661

Schoell, 1983

M. Schoell**Genetic characterization of natural gases**

American Association of Petroleum Geologists Bulletin, 67 (1983), pp. 2225-2238

Schwietzke et al., 2016

S. Schwietzke, O.A. Sherwood, L.M. Bruhwiler, J.B. Miller, G. Etiope, E.J. Dlugo kencky, S.E. Michel, V.A. Arling, B.H. Vaughn, J.W. White**Upward revision of global fossil fuel methane emissions based on isotope database**

Nature, 538 (2016), pp. 88-91

Seewald, 2003

J.S. Seewald**Organic–inorganic interactions in petroleum-producing sedimentary basins**

Nature, 426 (2003), pp. 327-333

Sherwood Lollar et al., 2008

B. Sherwood Lollar, G. Lacrampe-Couloume, K. Voglesonger, T. Onstott, L. Pratt, G. Slater**Isotopic signatures of CH_4 and higher hydrocarbon gases from Precambrian Shield sites: a model for abiogenic polymerization of hydrocarbons**

Geochimica et Cosmochimica Acta, 72 (2008), pp. 4778-4795

Stolper et al., 2014a

D. Stolper, A. Sessions, A. Ferreira, Neto E. Santos, A. Schimmelmann, S. Shusta, D.Valentine, J. Eiler**Combined ^{13}C–D and D-D clumping in methane: methods and preliminary results**

Geochimica Et Cosmochimica Acta, 126 (2014), pp. 169-191

Stolper et al., 2014b

D. Stolper, M. Lawson, C. Davis, A. Ferreira, E.S. Neto, G. Ellis, M. Lewan, A. M artini, Y.Tang, M. Schoell, A.L. Sessions, J.M. Eiler**Formation temperatures of thermogenic and biogenic methane**

Science, 344 (2014), pp. 1500-1503

Stolper et al., 2015

D. Stolper, A. Martini, M. Clog, P. Douglas, S. Shusta, D. Valentine, A. Session s, J. Eiler**Distinguishing and understanding thermogenic and biogenic sources of methane using multiply substituted isotopologues**

Geochimica et Cosmochimica Acta, 161 (2015), pp. 219-247

Stolper et al., in press

Stolper, D.A., Lawson, M., Formolo, M.J., Davis, C.L., Douglas, P.M.J., Sessions, A.L., Eiler, J.M., in press. The utility of methane clumped isotopes to constrain the origins of methane in natural gas accumulations. Geological Society of London Special Publications.

Strąpoć et al., 2011

D. Strąpoć, M. Mastalerz, K. Dawson, J. Macalady, A.V. Callaghan, B. Wawrik, C. Turich, M.Ashby**Biogeochemistry of microbial coal-bed methane**

Annual Review of Earth and Planetary Sciences, 39 (2011), pp. 617-656

Sugimoto and Wada, 1995

A. Sugimoto, E. Wada**Hydrogen isotopic composition of bacterial methane: CO_2/H_2 reduction and acetate fermentation**

Geochimica et Cosmochimica Acta, 59 (1995), pp. 1329-1337

Swain et al., 2008

M.R. Swain, G. Vasisht, G. Tinetti**The presence of methane in the atmosphere of an extrasolar planet**

Nature, 452 (2008), pp. 329-331

Takai et al., 2008

K. Takai, K. Nakamura, T. Toki, U. Tsunogai, M. Miyazaki, J. Miyazaki, H. Hiray ama, S.Nakagawa, T. Nunoura, K. Horikoshi**Cell proliferation at 122 °C and isotopically heavy CH_4 production by a hyperthermophilic methanogen under high-pressure cultivation**

Proceedings of the National Academy of Sciences, 105 (2008), pp. 10949-10954

Tang et al., 2000

Y. Tang, J. Perry, P. Jenden, M. Schoell**Mathematical modeling of stable carbon isotope ratios in natural gases**

Geochimica et Cosmochimica Acta, 64 (2000), pp. 2673-2687

Townsend-Small et al., 2012

A. Townsend-Small, S.C. Tyler, D.E. Pataki, X. Xu, L.E. Christensen**Isotopic measurements of atmospheric methane in Los Angeles, California, USA: influence of 'fugitive emissions'**

Journal of Geophysical Research: Atmospheres, 117 (2012), p. D07308

Truesdell et al., 1977

A.H. Truesdell, M. Nathenson, R.O. Rye**The effects of subsurface boiling and dilution on the isotopic compositions of Yellowstone thermal waters**

Journal of Geophysical Research, 82 (1977), pp. 3694-3704

Tsuji et al., 2012

K. Tsuji, H. Teshima, H. Sasada, N. Yoshida**Spectroscopic isotope ratio measurement of doubly-substituted methane**

Spectrochimica Acta Part A: Molecular and Biomolecular Spectroscopy, 98 (2012), pp. 43-46

Urey, 1952

H.C. Urey**On the early chemical history of the earth and the origin of life**

Proceedings of the National Academy of Sciences, 38 (1952), pp. 351-363

Valentine, 2011

D.L. Valentine**Emerging topics in marine methane biogeochemistry**

Annual Review of Marine Science, 3 (2011), pp. 147-171

Valentine et al., 2004

D.L. Valentine, A. Chidthaisong, A. Rice, W.S. Reeburgh, S.C. Tyler**Carbon and hydrogen isotope fractionation by moderately thermophilic methanogens**

Geochimica et Cosmochimica Acta, 68 (2004), pp. 1571-1590

Valentine and Reeburgh, 2000

D.L. Valentine, W.S. Reeburgh**New perspectives on anaerobic methane oxidation**

Environmental Microbiology, 2 (2000), pp. 477-484

Waldron et al., 1999

S. Waldron, J. Lansdown, E. Scott, A. Fallick, A. Hall**The global influence of the hydrogen iostope composition of water on that of bacteriogenic methane from shallow freshwater environments**

Geochimica et Cosmochimica Acta, 63 (1999), pp. 2237-2245

Waldron et al., 1998

S. Waldron, I.A. Watson-Craik, A.J. Hall, A.E. Fallick**The carbon and hydrogen stable isotope composition of bacteriogenic methane: a laboratory study using a landfill inoculum**

Geomicrobiology Journal, 15 (1998), pp. 157-169

Walter Anthony et al., 2012

K.M. Walter Anthony, P. Anthony, G. Grosse, J Chanton**Geologic methane seeps along boundaries of Arctic permafrost thaw and melting glaciers**

Nature Geoscience, 5 (2012), pp. 419-426

Wang et al., 2014

D.T. Wang, D.S. Gruen, P.L. Morrill, A. Rietze, K.H. Nealson, M.D. Kubo, D. Car dace, M.O.Schrenk, T.M. Hoehler, T.M. McCollom, G. Etiope, H. Hosgörmez, M. Schoell, S. Ono**New isotopic constraints on the sources of methane at sites of active continental serpentinization, American Geophysical Union 2014 Fall Meeting**

American Geophysical Union, San Francisco, CA (2014)

Wang et al., 2015

D.T. Wang, D.S. Gruen, Lollar B. Sherwood, K.-
U. Hinrichs, L.C. Stewart, J.F. Holden, A.N.Hristov, J.W. Pohlman, P.L. Morrill, M . Könneke, K.B. Delwiche, E.P. Reeves, C.N. Sutcliffe, D.J. Ritter, J.S. Seewald, J.C. McIntosh, H.F. Hemond, M.D. Kubo, D. Cardace, T.M. Hoehler, S. Ono**Non equilibrium clumped isotope signals in microbial methane**

Science, 348 (2015), pp. 428-431

Wang et al., 2016

D.T. Wang, P.V. Welander, S. Ono**Fractionation of the methane isotopologues $^{13}CH_4$, $^{12}CH_3D$, and $^{13}CH_3D$ during aerobic oxidation of methane by *Methylococcus capsulatus* (Bath)**

Geochimica et Cosmochimica Acta, 192 (2016), pp. 186-202

Wang et al., 2004

Z.G. Wang, E.A. Schauble, J.M. Eiler**Equilibrium thermodynamics of multiply substituted isotopologues of molecular gases**

Geochimica Et Cosmochimica Acta, 68 (2004), pp. 4779-4797

Webb and Miller, 2014

M.A. Webb, T.F. Miller III**Position-specific and clumped stable isotope studies: comparison of the Urey and path-integral approaches for carbon dioxide, nitrous oxide, methane, and propane**

Journal of Physical Chemistry A, 118 (2014), pp. 467-474

Webster et al., 2013

C.R. Webster, P.R. Mahaffy, S.K. Atreya, G.J. Flesch, K.A. Farley, O. Kemppinen, N.Bridges, J.R. Johnson, M. Minitti, D. Cremers**Low upper limit to methane abundance on Mars**

Science, 342 (2013), pp. 355-357

Webster et al., 2015

C.R. Webster, P.R. Mahaffy, S.K. Atreya, G.J. Flesch, M.A. Mischna, P.-Y. Meslin, K.A.Farley, P.G. Conrad, L.E. Christensen, A.A. Pavlov**Mars methane detection and variability at Gale crater**

Science, 347 (2015), pp. 415-417

Welhan, 1988

J.A. Welhan**Origins of methane in hydrothermal systems**

Chemical Geology, 71 (1988), pp. 183-198

Wen et al., 2015

T. Wen, M.C. Castro, B.R. Ellis, C.M. Hall, K.C. Lohmann**Assessing compositional variability and migration of natural gas in the Antrim Shale in the Michigan Basin using noble gas geochemistry**

Chemical Geology, 417 (2015), pp. 356-370

Whitehill et al., 2017

A.R. Whitehill, L.M.T. Joelsson, J.A. Schmidt, D.T. Wang, M.S. Johnson, S. Ono**C lumped isotope effects during OH and Cl oxidation of methane**

Geochimica et Cosmochimica Acta, 196 (2017), pp. 307-325

Whiticar, 1999

M.J. Whiticar**Carbon and hydrogen isotope systematics of bacterial formation and oxidation of methane**

Chemical Geology, 161 (1999), pp. 291-314

Whiticar et al., 1986

M.J. Whiticar, E. Faber, M. Schoell**Biogenic methane formation in marine and freshwater environments: CO_2 reduction *vs.* acetate fermentation—isotope evidence**

Geochimica et Cosmochimica Acta, 50 (1986), pp. 693-709

Wilhelms et al., 2001

A. Wilhelms, S. Larter, I. Head, P. Farrimond, R. di Primio, C. Zwach**Biodegradation of oil in uplifted basins prevented by deep-burial sterilization**

Nature, 411 (2001), pp. 1034-1037

Yeung et al., 2015

L.Y. Yeung, J.L. Ash, E.D. Young**Biological signatures in clumped isotopes of O_2**

Science, 348 (2015), pp. 431-434

Yeung et al., 2012

L.Y. Yeung, E.D. Young, E.A. Schauble**Measurements of $^{18}O^{18}O$ and $^{17}O^{18}O$ in the atmosphere and the role of isotope-exchange reactions**

Journal of Geophysical Research: Atmospheres, 117 (2012), p. D18306

Yoshinaga et al., 2014

M.Y. Yoshinaga, T. Holler, T. Goldhammer, G. Wegener, J.W. Pohlman, B. Brun ner, M.M.Kuypers, K.-U. Hinrichs, M. Elvert**Carbon isotope equilibration during sulphate-limited anaerobic oxidation of methane**

Nature Geoscience, 7 (2014), pp. 190-194

Young et al., 2017

Young, E., Kohl, I., Sherwood Lollar, B., Etiope, G., Rumble, D., Li, S., Haghnegahdar, M., Schauble, E., McCain, K., Foustoukos, D., Sutclife, C., Warr, O., Ballentine, C., 2017. The relative abundances of resolved CH_2D_2 and $^{13}CH_3D$ and mechanisms controlling isotopic bond ordering in abiotic and biotic methane gases. Geochimica et Cosmochimica Acta 203.

Young et al., 2016

E.D. Young, D. Rumble, P. Freedman, M. Mills**A large-radius high-mass-resolution multiple-collector isotope ratio mass spectrometer for analysis of rare isotopologues of O_2, N_2, CH_4 and other gases**

International Journal of Mass Spectrometry, 401 (2016), pp. 1-10

Zhang et al., 2011

S. Zhang, H. Huang, Z. Feng, Y. Shuai**Geochemical characterization of secondary microbial gas occurrence in the Songliao Basin, NE China**

Organic Geochemistry, 42 (2011), pp. 781-790

Zhang and Krooss, 2001

T. Zhang, B.M. Krooss**Experimental investigation on the carbon isotope fractionation of methane during gas migration by diffusion through sedimentary rocks at elevated temperature and pressure**

Geochimica et Cosmochimica Acta, 65 (2001), pp. 2723-2742